Elsevier Editorial System(tm) for Quaternary Science Reviews
Manuscript Draft

Manuscript Number: JQSR-D-14-00067R2

Title: Vegetation and environmental responses to climate forcing during the last glacial maximum and deglaciation in the East Carpathians: attenuated response to maximum cooling and increased biomass burning

Article Type: Special Issue: 4th INTIMATE

Keywords: LGM, Romania, pollen, XRF, magnetic susceptibility, biomass burning, grass steppe

Corresponding Author: Dr. Eniko Magyari, PhD

Corresponding Author's Institution: MTA-MTM-ELTE

First Author: Eniko Magyari, PhD

Order of Authors: Eniko Magyari, PhD; Daniel Veres, PhD; Volker Wennrich, PhD; Bernd Wagner; Mihály Braun, PhD; Gusztáv Jakab, PhD; Dávid Karátson, PhD; Gyöngyvér Ferenczy; Zoltán Pál, PhD; Guillaume St-Ogne, PhD; Janet Rethemeyer, PhD; Jean-Pierre Francois; Frederik von Reumont, PhD; Frank Schäbitz, PhD

Abstract: The Carpathian Mountains were one of the main mountain reserves of the boreal and cool temperate flora during the Last Glacial Maximum (LGM) in East-Central Europe. Previous studies demonstrated late glacial vegetation dynamics in this area; however, our knowledge on the LGM vegetation composition is very limited due to the scarcity of suitable sedimentary archives. Here we present a new record of vegetation, fire and lacustrine sedimentation from the youngest volcanic crater of the Carpathians (Lake St Anne, Lacul Sfânta Ana, Szent-Anna-tó) to examine environmental change in this region during the LGM and the subsequent deglaciation. Our record indicates the persistence of boreal forest steppe vegetation (with Pinus, Betula, Salix, Populus and Picea) in the foreland and low mountain zone of the East Carpathians and Juniperus shrubland at higher elevation. We demonstrate attenuated response of the regional vegetation to maximum global cooling. Between ~22,870 and 19,150 cal yr BP we find increased regional biomass burning that is antagonistic with the global trend. Increased regional fire activity suggests extreme continentality likely with relatively warm and dry summers. We also demonstrate xerophytic steppe expansion directly after the LGM, from ~19,150 cal yr BP, and regional increase in boreal woodland cover with Pinus and Betula from 16,300 cal yr BP. Plant macrofossils indicate local (950 m a.s.l.) establishment of Betula nana and B. pubescens at 15,150 cal yr BP, Pinus sylvestris at 14,700 cal yr BP and Larix decidua at 12,870 cal yr BP. Pollen data furthermore support population genetic inferences regarding the regional presence of some temperate deciduous trees during the LGM (Fagus sylvatica, Corylus avellana, Fraxinus excelsior). Our sedimentological data also demonstrate intensified aeolian dust accumulation between 26,000 and 20,000 cal yr BP.

Highlights (for review)

A multi-proxy record from the E Carpathians dating to the LGM & deglaciation

Evidence for LGM persistence of boreal forest steppe and *Juniperus* shrubland

Increased biomass burning between 22,870 and 19,150 cal yr BP

Xerophytic steppe expansion from ~19,150 cal yr BP

Vegetation and environmental responses to climate forcing during the last glacial maximum and deglaciation in the East Carpathians: attenuated response to maximum cooling and increased biomass burning

Magyari[1], E. K., Veres[2], D., Wennrich[3], V., Wagner[3], B., Braun[4], M., Jakab[5], G., Karátson[6], D., Pál[7], Z., Ferenczy[1], Gy., St-Onge[8], G., Rethemeyer[3], J., Francois, J-P[9]., von Reumont[9], F., Schäbitz[9], F.

[1]MTA-MTM-ELTE Research Group for Paleontology, Eötvös University, Pázmány Péter stny. 1/C, H-1117 Budapest, Hungary
[2]Institute of Speleology, Romanian Academy, Clinicilor 5, 400006 Cluj-Napoca, Romania
[3]Institute of Geology and Mineralogy, University of Cologne, 6Zülpicher Str. 49a, 50674 Cologne, Germany
[4]Hertelendi Laboratory of Environmental Studies, Institute of Nuclear Research of the Hungarian Academy of Sciences, H-4001 Debrecen, P. O. Box 51, Hungary
[5]Institute of Environmental Sciences, Szent István University, H-5540 Szarvas, Szabadság út 1-3, Hungary
[6]Eötvös University, Department of Physical Geography, H-1117 Budapest, Pázmány s. 1/C, Hungary
[7]Department of Physical Geography in Hungarian Language, Faculty of Geography, Babes Bolyai University of Cluj, Str. Clincilor No. 5–7, 3400 Cluj-Napoca, Romania
[8]GEOTOP-UQAM, Montreal, QC, Canada
[9] Seminar of Geography and Education, University of Cologne, Gronewaldstr. 2, D-50931 Cologne, Germany

Abstract

The Carpathian Mountains were one of the main mountain reserves of the boreal and cool temperate flora during the Last Glacial Maximum (LGM) in East-Central Europe. Previous studies demonstrated late glacial vegetation dynamics in this area; however, our knowledge on the LGM vegetation composition is very limited due to the scarcity of suitable sedimentary archives. Here we present a new record of vegetation, fire and lacustrine sedimentation from the youngest volcanic crater of the Carpathians (Lake St Anne, Lacul Sfânta Ana, Szent-Anna-tó) to examine environmental change in this region during the LGM and the subsequent deglaciation. Our record indicates the persistence of boreal forest steppe vegetation (with *Pinus*, *Betula*, *Salix*, *Populus* and *Picea*) in the foreland and low mountain zone of the East Carpathians and *Juniperus* shrubland at higher elevation. We demonstrate attenuated response of the regional vegetation to maximum global cooling. Between ~22,870 and 19,150 cal yr BP we find increased regional biomass burning that is antagonistic with the global trend. Increased regional fire activity suggests extreme continentality likely with relatively warm and dry summers. We also demonstrate xerophytic steppe expansion directly after the LGM, from ~19,150 cal yr BP, and regional increase in boreal woodland cover with *Pinus* and *Betula* from 16,300 cal yr BP. Plant macrofossils indicate local (950 m a.s.l.) establishment of *Betula nana* and *B. pubescens* at 15,150 cal yr BP, *Pinus sylvestris* at 14,700 cal yr BP and *Larix decidua* at 12,870 cal yr BP. Pollen data furthermore support population genetic inferences regarding the regional presence of some temperate deciduous trees during the LGM (*Fagus sylvatica*, *Corylus avellana*, *Fraxinus excelsior*). Our sedimentological data also demonstrate intensified aeolian dust accumulation between 26,000 and 20,000 cal yr BP.

Keywords: LGM, Romania, pollen, XRF, magnetic susceptibility, biomass burning, grass steppe, boreal and temperate tree refugia

1. Introduction

Phylogeographical (Fér et al., 2007; Ronikier et al., 2008a,b, 2011; Bálint et al., 2011), floristic (Tasenkevich, 1998) and paleovegetational studies (Tanţău et al., 2006; Feurdean et al., 2004, 2012a,b, 2013a) suggest that the diverse, endemic-rich modern flora of the Carpathians closely reflects the exceptionally varied topography and diverse meso- and macroclimate of the mountains that provided suitable habitat for temperate, boreal and alpine plants throughout the Quaternary. How the regional biomes evolved through the high amplitude climatic fluctuations of the Late Quaternary needs however further research, as existing well-dated and high-resolution studies from the Romanian Carpathians provide insight mainly into the vegetation dynamics of the late glacial (Feurdean et al., 2007, 2012, 2014; Magyari et al., 2012) and Holocene (Fărcaş, 1999, 2013; Tanţău et al., 2003, 2006, 2011; Feurdean and Bennike, 2004; Magyari et al. 2009; Feurdean et al., 2011, 2013a). Knowledge on the last glacial maximum (LGM) (19,000-26,000 cal yr BP according to Clark et al., 2009 and corresponding to Greenland isotope chronostratigraphic events GS-3, GI-2.2, GS-2.2, GI-2.1, GS-2.1bc as defined in Rasmussen et al., 2014) vegetation composition is however still very limited (Tanţău et al., 2006; Obidowicz, 2006; Jankovská and Pokorný, 2008; Kuneš et al., 2008; Feurdean et al., 2014). This is due to the scarcity of sites that preserve sediments suitable for pollen and plant macrofossil analysis from this period. Therefore, several important research questions await answers regarding the LGM vegetation changes in this region, such as 1) how terrestrial vegetation responded to the millennial-scale stadial/interstadial climate fluctuation of marine isotope stage 2 (e.g. GI-2.1 and GI-2.2; Rasmussen et al., 2014); 2) what temperate and boreal woody species survived the LGM locally at mid altitudes; 3) how the LGM vegetation composition of the mountain zone compared with the surrounding lowlands both west (Magyari et al., 1999, 2014; Sümegi et al., 2013) and east (Markova et al., 2009) of the Carpathians; and finally 4) if there is any causal relationship between hydrological changes in the Black Sea water column and catchment area (Major et al., 2006; Rostek and Bard, 2013; Soulet at al., 2013) and the nearby Carpathian region. The distance between Lake St Anne and the Black Sea is c. 300 km and the weather systems of the two areas are strongly connected to each other.Therefore, it is reasonable to assume that climatic changes recorded in the Black Sea sediments, i.e. the 19,000 cal yr BP temperature increase, or the presence of *Sphagnum* derived alkenones from ca. 17,000 cal yr BP likely denote important boundaries when major ecosystem responses are also expected in the Carpathians. For example, a recent lipid biomarker study on marine sediments from the NW Black Sea basin concluded that permafrost melt and peatland development in the North European and Russian Plains were initiated directly after the final retreat of the Scandinavian Ice sheet from the Russian Plain, already during Heinrich stadial 1 (~17,000 cal yr BP) (Rostek and Bard, 2013). At the same time, the Sofular cave (south of Black Sea) $\delta^{13}C$ record suggests significant regional moisture increase (Göktürk et al., 2011). These changes show up in both records just as prominently as the onset of the late glacial interstadial (GI-1e; Blockley et al., 2012). An interesting question is thus how the terrestrial ecosystem in the Carpathian area has reacted to Scandinavian ice melt and how the Black Sea hydrological change influenced the climate system in the Carpathians, if at all. Can we detect vegetation change in the Carpathian Mountains connectable to moisture availability increase in this period? Another provoking feature of the East and Central European lowlands during the LGM is the presence of a clear latitudinal decrease in available moisture that resulted in a well-developed zonation ranging from tundra and boreal forest in the north to steppe to semi-desert to the south, over the Russian Plain (Markova et al., 2009). A similar picture is now emerging in the lowlands of East-Central Europe, west and south of the Romanian Carpathians (Feurdean et al., 2014). With its latitude 46°7′35″N and altitude 946 m above sea level (a.s.l.), Lake St Anne lies in the boreal forest steppe zone of the LGM vegetation reconstructions, so we expect a considerable input of regional pollen from this vegetation unit. A straightforward question is thus how the mid-elevation (around 1000 m a.s.l.) mountain pollen assemblages differ from the lowlands at similar latitudes especially given that during the Holocene, the Carpathians acted as an orographic barrier for regional hydroclimate influences (Drăguşin et al., 2014). It is therefore interesting to test whether changes could be identified in vegetation and climate patterns in the region following the inferred latitudinal displacement of the atmospheric circulation patterns in Europe in pace with the millennial-scale climate change events (Moreno et al., 2011). On the other hand, climate model simulations (Renssen and Isarin, 2001; Strandberg et al., 2011; Huntley et al., 2013), and niche modelling studies (Svenning et al., 2008) suggest considerably lower amplitude summer and winter temperature fluctuation during GS-2.1 in East-Central Europe than in Western Europe, with annual temperature decreasing by ~9 ^{o}C (Varsányi et al., 2011) and precipitation by maximum 60% relative to modern values (Heyman et al., 2013). Therefore the conditions were potentially much favourable for the survival of temperate floristic elements at latitudes >45^{o} N in East-Central Europe compared to Western Europe. Although the question of cryptic northern temperate tree refugia is still hotly debated and sometimes rejected (Willis et al., 2000; Stewart and Lister, 2001; Willis and van Andel, 2004; Provan and Bennet, 2008; Tzedakis et al., 2013; Huntley at al., 2013; Feurdean et al., 2013b), an increasing number of phylogeographical studies on temperate animal species supports northerly refugia in the Carpathian Mountains and likely also on the surrounding lowlands drained by several large river valleys (summarized in Schmitt and Varga, 2012). In this study we use the term cryptic refugia for temperate plant species that likely occurred at mid-elevations in the Carpathian Mountains. If present, their small populations were likely situated north of the species main glacial distribution range (Provan and Bennett, 2008). New paleoevegetation and paleoenvironmental data from this under-investigated area can thus provide important insights into these scientific issues. Here we attempt answering these questions through a multi-proxy study of a new sediment sequence from Lake St Anne in the East Carpathian Mountains, Romania (Figure 1). This paper contributes to the aims of INTIMATE (INTegrating Ice core, MArine, and TErrestrial records) by providing a new, high resolution vegetation record for the LGM and subsequent deglaciation from a seriously underinvestigated area. This data is important for climate modelers within the INTIMATE community to test the performance of climate models and thereby reduce the uncertainty of future predictions (Renssen and Osborn, 2003; Jost et al., 2005).

2. Glacial environments in the Romanian Carpathians

Compared to the Alps, mountain glaciation in the Carpathian Mountains was less extensive. In the Romanian Carpathians development of glaciers was confined to massifs exceeding 1600 m elevation. Recent glacial geomorphological studies suggest that maximum glacier extent pre-dated the LGM (Urdea, 2004; Urdea et al., 2011). Apparently, the glacial equilibrium line altitude (ELA, broadly equals the snowline) was lower in the north (~1500 m) than in the south (1700-1800 m), and a secondary W-E trend was also identified, with lower altitude ELA in the west suggesting more precipitation in the western side of the E Carpathians where Lake St Anne lies (Figure 1). Indeed, geomorphological investigations suggest a predominantly westward air mass circulation during the last glaciation in the Romanian Carpathians (Mîndrescu et al., 2010). Exposure ages from the Retezat and Parang Mts suggest that glacial advance in these mountain chains post-dated the LGM and occurred at 16,800 ± 1800 and 17,900 ± 1600 cal yr BP. Notable is the coincidence of these glacier advances with the final melting of the Scandinavian Ice sheet in the Russian Plain that resulted in increased water discharge to the Black Sea (Soulet et al., 2013) and likely contributed to intensified vapour circulation and precipitation in the Carpathians during the second part of Heinrich stadial 1, at ca. 17,000 cal yr BP. Maximum permafrost extension coincided with maximum northern ice sheet extent, permafrost reached as far south as 47°N with discontinuous permafrost down to 45^{o} N (Vanderberghe et al., 2012; Fábián et al., 2013). In the Harghita Mts periglacial landforms and permafrost features are well-known (Naum and Butnaru, 1989), but in the area of Lake St Anne no glaciers were developed.

3. Study site

Lake St Anne (Lacul Sfânta Ana; Szent-Anna tó; 946 m a.s.l.; 46° 07′ 35″ N, 25° 53′ 17″ E) is situated in the Ciomadul Massif of the Harghita Mts (Figure 1). This area hosts the youngest eruptive volcanic activity in East-Central Europe. Radiometric dating of the youngest tephra suggests that the St Anne (Sfânta Ana) crater was likely formed during late MIS3, sometimes between 26,000-33,000 cal yr BP (Harangi et al., 2010; Karátson et al., 2013). The Ciomadul volcano is a dacitic lava dome complex consisting of a central edifice truncated by the twin craters of Lake St Anne and Mohoş, and surrounded by a number of individual lava domes, as well as a narrow volcaniclastic ring plain (Figure 1). The mid-elevation hills (700-900 m, highest peak 1301 m a.s.l.) rise above the Lower Ciuc Basin (700 m a.s.l.), which is located to the north (Figure 1b). Post-volcanic activity is present in the form of CO_2 degassing and mofettas (Szakács et al., 2002); degassing shows varying intensity in the St Anne crater. Geologically the volcano is considered to be still active (Popa et al., 2011), which is unique in East-Central Europe.

The crater lake has been formed between dacitic lava dome as well as pyroclastic rocks, both being poor in calcium. The predominant soil type is acidic, non-podzolic, brown earth at heights of below 900 m a.s.l., while andosols (dark soils with high organic content and traces of podsolization) are generally formed above this height on young volcanic rocks (Jakab et al., 2005; Jakab, 2011).

The area of the lake is ~ 189900 m^2; maximum water depth is ~6 m, mean depth is ~3.1 m, mean width is ~310 m (Pandi, 2008). The lake water is neutral (summer) to acidic (winter); pH is between 4 and 7.3; summer pH has increased considerably in recent years due to human impact (Pál 2001; Magyari et al., 2009). Today the crater slope is covered by mixed *Fagus sylvatica* and *Picea abies* forest; the latter species is more abundant on shaded locations and on the lake shore. *Carpinus betulus*, *Betula pendula*, *Salix caprea Salix cinerea, Acer platanoides*, and *Pinus sylvestris* appear as admixtures in the crater slope forest. In the shallow NE corner of the lake a floating fen develops (Pál, 2000). Its main constituents are *Carex rostrata*, *C. lasiocarpa*, *Sphagnum angustifolium* and *Lysimachia thyrsiflora*. A typical feature of the crater and also the nearby Olt river valley is the phenomenon of thermal inversion, which results in reversed order vegetation zonation; deciduous forests on higher slopes are often underlain by *Picea abies* forests in the river valleys and in closed basins. The area belongs to the East Carpathian floristic province that abounds in alpine endemic and relict plants (~200 species). In the Transylvanian Basin and in the piedmont area the potential vegetation is oak forest up to 700 m, which is however fragmented due to historic deforestation. Oak forests are mainly replaced by hay meadows, pastures and crop fields. Beech forest grows between 700-1100 m, and spruce forest above 1100 m.

The climate is temperate continental. Annual mean temperature at the elevation of the crater is 6-7 ^{o}C; January means range between -5 to -6 ^{o}C. The warmest month is July, with mean temperature ~15 ^{o}C. Annual precipitation is 800 mm. Prevailing winds come from the west and north-west, with a frequency above 50% (Diaconu and Mailat, 2010).

Lake St Anne is a medium sized lake meaning that approximately ~50 % of its incoming pollen rain is of regional source, while local and extra-local pollen make up the other ~50% (Sugita, 2007). Note however that the pollen source area of the lake likely varied considerably through time, especially between forested periods (Holocene) and periods when the surroundings of the lake were not forested (LGM, for example). In unforested periods the pollen source area was likely much larger.

Materials and methods

3.1. Drilling

The sediment of Lake Saint Anne was sampled during the winter of 2010 using a 7-cm-diameter Livingstone piston corer with a chamber length of 200 cm (core SZA-2010). The borehole was cased down to 1200 cm depth. At this core location, drilling started at 600 cm water depth and reached 1700 cm (including water-depth). The basal sediment was claysilt with dropstones. The 2010 core used in this study has not reached the bottom of the lake sedimentary succession wrapping the volcanic rocks. We returned to the site in 2013 and obtained a new core (core SZA-2013) that reached the bottom of the lake sediment at approximately 2100 cm; under this depth pumice gravel alternates with sandy silt down to 2300 cm, followed by coarse pumice gravel.

3.2. Radiocarbon dating

Radiocarbon dating was the main method used to establish an age-depth model for the sediment sequence SZA-2010. Material for radiocarbon dating was selected from 10 horizons, and comprises plant macrofossils and charcoal down to 1127 cm sediment depth. Below 1340 cm Cladocera eggs and chironomid head capsules were also used for dating since either no, or very few terrestrial macrofossils were found. All samples were pretreated according to Rethemeyer et al. (2013), but using shorter treatment times with acid and alkali to avoid loss of the very small plant fragments, and samples were graphitized at Cologne University. The graphite targets were measured by accelerator mass spectrometry (AMS) at ETH in Zurich, Switzerland (Table 1). The radiocarbon ages of all samples were converted into calendar ages reported in years before present (cal yr BP) using the INTCAL13 calibration curve (Reimer et al., 2013).

3.3. Physical and chemical proxies

The analytical work presented here focuses on the 950-1700 cm sediment section of core SZA-2010, which comprises the LGM, late glacial and early Holocene. Individual core segments were split into two halves in the laboratory. Subsequently, one core half was photographed, described, and used for

MSCL core logger derived magnetic susceptibility at 5-mm resolution, and high-resolution X-ray fluorescence (XRF) scanning. The XRF scanner (ITRAX core scanner; COX Ltd., Sweden) was equipped with a Cr-tube set to 30 kV and 30 mA, and a Si-drift chamber detector (Croudace et al., 2006). XRF scanning was performed at a resolution of 2 mm and an analysis time of 20 s per measurement. The obtained count rates for individual elements can be used as semi-quantitative estimates of their relative concentrations. Only a selection of elemental data from the XRF scanning is presented here.

The other core half was continuously cut at 1 cm intervals and stored in self-sealing bags. For grain-size analysis, 20 raw sediment samples with a dry weight of 1 g each were selected at 20 cm intervals between 1100-1700 cm. Grain-size analysis on the clastic fraction was carried out after removing the >630 μm fraction by sieving and using a Micromeritics Saturn DigiSizer 5200 laser particle analyser. The volume percentages (vol %) of the individual grain-size fractions were calculated from the average values of 3 runs.

3.4. Biological proxies

Pollen analysis was carried out on 107 samples taken at 2-8 cm intervals. 2 cm^3 wet sediment was treated with HCl, NaOH, HF and acetolysis and sieved between the 180 and 10 micron fractions (Bennett and Willis, 2001). Identification of pollen and other palynomorphs was performed with relevant keys and atlases (Moore et al., 1992; Reille, 1995, 1998, 1999; Beug, 2004). The relative percentages of pollen taxa and non-pollen palynomorphs (NPP) are based upon the sum of terrestrial pollen (excluding aquatics, spores and algae). A minimum of 500 pollen grains were counted per sample (except for two samples, where 350 terrestrial pollen were counted due to low pollen concentration). Pollen accumulation rates (PAR) were calculated using the pollen concentrations that were divided by the sediment deposition times inferred by the linear age-depth model. PAR was used to infer past plant population size changes (Seppä and Hicks, 2006). Microcharcoal was counted on the pollen slides. All particles > 10 micron were enumerated, and the results were expressed as microcharcoal accumulation rates in addition to pollen accumulation rates. For the reconstruction of major vegetation types pollen taxa were grouped into ecological types following the protocol of Feurdean et al. (2014). The 6 main plant types were: coniferous, cold deciduous trees, temperate deciduous taxa, warm temperate taxa, warm /dry steppe, and other grassland and dry shrubland (Supplementary Table 1).

The presence of plant macrofossils was first tested in several large volume sediment samples, of which twelve were studied in detail. These 15 cm^3 sediment samples were soaked in 10% NaOH for

30 minutes, heated at 70 ^{o}C and subsequently sieved through a 250 µm mesh. In these samples macrocharcoal and identifiable plant macrofossils were tallied.

3.5. Data analysis

Local pollen assemblage zones were defined using stratigraphically constrained cluster analysis (CONISS; Birks and Gordon, 1985) as implemented in the program Psimpoll 3.00 (Bennett, 2007). The analysis was performed using all terrestrial taxa (excluding ferns) that reached 5% at least in one sample, following re-calculation of the dataset to proportions. Rarefraction analysis was used to infer changes in palynological diversity or richness using the software Psimpoll 3.00 (Bennett, 2007). Ordination analysis was carried out on the pollen data to facilitate interpretation of the vegetation shifts. To estimate the linearity of the latent gradients in the data, detrended correspondence analysis (DCA) was carried out. The longest DCA axis gradient length was <2.0 standard deviation units, and thus the linear ordination method (principal component analysis, PCA) was chosen (Legendre and Birks, 2012). PCA was performed on the covariance matrix following square-root-transformation of the percentages pollen data. Only terrestrial taxa with values exceeding 5% at least in one sample were included in this analysis.

Detrended canonical correspondence analysis (DCCA) was used to determine the amount of palynological change along time (turnover) that is a reliable statistical tool to estimate changes in floristic composition within a landscape (Birks and Birks, 2008). This analysis uses age as the external constraint (Birks, 2007). An age–depth file is uploaded as environmental data. Results were scaled in SD units (units of species standard deviations), and changes in pollen composition for the LGM, late glacial and early Holocene were estimated by looking at the range of sample scores on the first, time-constrained DCCA axis, where each value represents a position of a pollen sample relative to the entire gradient scale. Thus, larger variation in the sample scores within a sequence implies greater compositional changes. Ordinations were performed with Canoco 5.

4. Results

4.1. Age-depth models

Table 1 lists all radiocarbon dates obtained from core SZA-2010. Generally, but particularly in the lowermost 2 samples, the sample dry weights were very small (1-5 mg) resulting in relatively low amounts of carbon (90-180 µg) available for graphitization. In addition, all radiocarbon dates below 1340 cm were measured partly on aquatic remains, which may include reservoir effect. Given the volcanic origin of the lake and the varying intensity of CO_2 upwelling that might bring old carbon into the water column, we may expect an ageing effect in the results below 1340 cm. Taking these potential problems into account, the results are reassuring in that they show only one age reversal at 1091-1092 cm. This sample yielded an older age (15,400±44 yr BP) than the one below and above it (14,038±38, 14,541±67 years BP). Facing these facts, we used two different methods to examine age-depth relationship in the core. As shown in Figure 2a, the Bayesian method (Blaauw, 2013) identifies one outlier and suggests fast and nearly linear sediment accumulation between 1700 and 1072 cm (26,400 - 16,100 cal yr BP, deposition time: 12-44 yr cm^{-1}), followed by much slower sediment accumulation above, that is again close to linear until 980 cm (16,100 - 7200 cal yr BP; deposition time: 70-124 yr cm^{-1}). In an alternative age-depth model we used linear interpolation (Figure 2b) and excluded two radiocarbon dates on the basis of the pollen stratigraphy and XRF data (1073 cm: 14038±38 yr BP, 1092 cm: 15400±44 yr BP). Both records suggested that these post LGM radiocarbon dates that were measured on terrestrial sediment components are probably too old. The Bayesian model (which takes into account all dates) suggest the first increase in *Pinus* pollen at 17,000 cal yr BP and a rapid decreases in Ti and Al counts even earlier, at 17,500 cal yr BP. Although we cannot exclude that these warming indicator events took place as early as Heinrich stadial 1 (GS-2.1a in NGRIP, Rasmussen et al., 2014), we can also assume the presence of re-deposited old carbon in these samples, which were deposited at the time of active melting on the crater slope and during major ecosystem-reorganisation. The linear model differs from the Bayesian model between 12,000 and 18,000 cal yr BP; in this period the linear model shows younger ages. Particularly, the timing of xerophytic steppe increase (mainly *Artemisia* and *Chenopodim*-type) agrees better with the timing of the Younger Dryas stadial (GS-1) in the NGRIP record (Figure 3). For these reasons, we chose the linear age-depth model and present our results along this timescale.

4.2. Sediment stratigraphy, grain size, magnetic susceptibility, selected XRF data, LOI

Figure 3, Supplementary Table 2 and Supplementary Figure 2 show the major physical and chemical characteristics and lithostratigraphy of core SZA-2010. Based on the sediment stratigraphy, the core is characterised by coarse peaty gyttja (Unit I) with very high organic content (>80%) between 950-977 cm, followed by clayey silty gyttja down to 1036 cm (Unit II; LOI: 30-80%). Silt becomes the dominant sediment component in the late glacial (Unit 3; 1036-1100 cm) that is separated by the LGM silt rich sediments by its more yellowish colour and by the absence of distinct pumice gravel layers (LOI: 5-30%). The yellowish colour of this sediment unit is likely attributable to Fe(III) compounds, while black mottling may represent FeS precipitation. The LGM section of the core (Unit IV) shows frequent alternation among dark and light grey and occasionally laminated silt rich sediments with very low organic content (2-5%). Vivianite precipitates (large patches) are abundant between 1582-1617 cm suggesting reducing conditions in the top sediment layer, phosphorous availability (likely from decaying organic matter) and abundant ferrous ions in the sediment (Manning et al., 1991). Dropstones (pumice gravels) with sizes 5-40 mm appear frequently in sediments below 1090 cm. Some layers in unit IV resemble turbidites with dark coloured bottom horizon overlain by coarser, sand-rich sediment gradually grading into silt-rich lighter coloured sediment. Since these turbidite-like strata are thin and infrequent, often miss grain-size grading, and do not show different pollen, chemical composition and organic content, we have not cut them out from the sediment stratigraphy.

Magnetic susceptibility (MS) readings are characterised by high and fluctuating values between 1300-1700 cm (20,140-26,850 cal yr BP) suggesting variations in the abundance of magnetic minerals and rapid changes in sediment environmental magnetic characteristics until ca. 20,140 cal yr BP. This is followed by a stepwise decrease in MS, and gradually decreasing values were recorded towards the top of the sequence. Notable is that the MS record does not show a strong correlation with the Fe record suggesting that concentration changes of Fe do not explain changes in MS. MS fluctuation therefore likely correlate with changes in the composition of the allochtonous sediment components, overprinted by syn- and postsedimentary redox changes as suggested by the presence of vivianite in the sediment. Preliminary rock-magnetic results suggest that the main magnetic carrier is magnetite, and only some of the sharp increases in MS values reflect the presence of hematite. Furthermore, low MS values usually characterise sediment with high water and organic matter contents, indicating that dilution effects in highly organic sediments substantially influence MS readings.

Titanium, an element indicative of detrital input into the basin (Kylander et al., 2011) shows high values in the LGM and late glacial part of the sequence; the first decline is detected at 1100 cm (16,150 cal yr BP) followed by declining and fluctuating values during the late glacial. The final decrease in these clastic-associated elements occurs at 1035 cm (12,460 cal yr BP).

In the GS-3 and GS-2 part of the sequence, between 1700 and 1094 cm (26,850-15,810 cal yr BP), loss-on-ignition inferred organic contents are very low, below 5% (av. 4%). This is followed by gradual increase to 12% at 1080 cm (15,040 cal yr BP). At this depth/time a step-wise increase is detected in LOI; values increase from 12% to 32% between 1080 and 1051 cm (15,040-13,430 cal yr BP). The highest value is 36% at 1067 cm (14,320 cal yr BP). This is followed by a short decrease in LOI between 1051 and 1037 cm (13,430-12,650 cal yr BP). In the same period Al and Ti values increase, while AP decrease. This short reversal in LOI is followed by steep increase from 1037 cm; organic contents increase to c. 80% by 1011 cm (10,150 cal yr BP) and such high values characterise the sediment up to 950 cm.

Overall, the comparison of the MS, LOI and XRF records (Figure 3) suggests that the sediment section between 1051 and 1031 cm likely corresponds with the GS-1 climatic reversal (Rasmussen et al., 2014). The linear age-depth model places this interval between 13,430 and 12,650 cal yr BP that is ~530 years earlier than the same period in the NGRIP event stratigraphy, between 12,896-11,703 cal yr BP (Blockley et al., 2012). This suggests that the linear age-depth model is likely biased in the lateglacial sediment section.

4.3. Pollen, algae, non-pollen palynomorphs (NPP) and microcharcoal

Percentage and accumulation rates of selected pollen and spore types are displayed in Figures 4, 5, 6 and Supplementary Figure 3; the main characteristics of each pollen assemblage zones as defined by CONISS are discussed in Table 2. Zones SZA 1-4 represent the LGM and late glacial, while SZA-5 and SZA-6 date to the Holocene; their pollen and plant macrofossil composition were discussed in Magyari et al. (2006, 2009). Inferred terrestrial and aquatic vegetation changes are also discussed in Table 2; of these changes climatically and ecologically the most important are the following.

Dry/cold continental steppe herbs, such as *Artemisia* and *Chenopodium*-type are the most abundant in SZA-1 (26,350-22,870 cal yr BP) and SZA-3 (19,150-14,600 cal yr BP) pointing to the expansion of xerophytic steppe against grass steppes in these periods. Maximum development of xerophytic steppes dates between 1230-1033 cm (19,150-12,300 cal yr BP) on the basis of the pollen influx values.

Palynological richness, which is a measure of past regional vegetation diversity, displays the highest values within the LGM, in zone SZA-2, with peak values between 20,000-22,000 cal yr BP. This diversity is mainly attributable to increased diversity of arctic/alpine herbs (Figure 4, Table 2).

Pinus, *Juniperus* and Poaceae are the most abundant pollen types in the LGM pollen zones (SZA-1 to SZA-3). Arboreal pollen percentages are relatively high (av. 45%) in this period.

Thalictrum shows two prominent percentage peaks at 1526 and 1243 cm (23,350 and 19,320 cal yr BP); both precede important changes in the terrestrial pollen composition indicated by pollen zone boundaries between SZA-1-2 and SZA-2-3 (Figure 4). Although species-level identification in light microscope is not possible within this genus; the modern distribution of *Thalictrum* species in the Carpathian region suggests that the most eurithermic, widespread and wet ground species is *Thalictrum lucidum* that is a typical element of waterside tall forb communities. Its increased representation therefore likely indicates changes in the water level or permafrost conditions.

The pollen accumulation rate (PAR) diagram is presented (Figure 6) to examine changes in terrestrial vegetation cover during the LGM, late glacial and Holocene. Provided that our timescales approximate changes in past sediment accumulation rates well, PAR values should be indicative of past population size and/or pollen productivity changes of terrestrial plants (Seppä and Hicks, 2006). Generally, PAR values are the lowest in SZA-1 suggesting low overall vegetation cover; relatively high Poaceae PARs suggest that grass-steppes likely reached their largest coverage during SZA-2; while increased *Artemisia* and *Chenopodium*-type PARs suggest that a major increase in xerophytic steppe, semi-desert cover appeared in SZA-3 and SZA-4. This was followed by *Pinus*, *Betula* and *Picea* PAR increases in SZA-4 suggesting increasing population sizes of boreal forest trees during the late glacial. Total terrestrial pollen accumulation rates (Figure 4) furthermore suggest that pollen productivity and in connection with this likely overall vegetation cover in the vicinity of Lake St Anne was very low between 26,350 and 13,300 cal yr BP and increased rapidly afterwards.

Strongly fluctuating PAR values in the late glacial and early Holocene pollen assemblage zones (SZA-4 to SZA-6) suggest that sediment accumulation rates are likely much more variable than we see in the age-depth model. This is indicated by common PAR peaks in case of all taxa, e.g. at 1010, 1040, 1073 cm depth.

Microcharcoal accumulation rates varied strongly in the sequence. Most notable is the increase in SZA-2 and SZA-4 suggesting increased regional fire activity in both periods.

4.4. Plant macrofossils

Table 3 lists terrestrial plant species and some mosses identified in the GS-2, GI-1 and GS-1 sections of core SZA-2010 on the basis of studying twelve large volume samples (15 cm^3 each). High-resolution plant macrofossil analysis of the late glacial section of this core is underway, and the results of this analysis will be published in a separate paper. As mentioned in the radiocarbon dating section, the GS-3 and most GS-2 section of the core was devoid of terrestrial plant macrofossils suggesting sparsely vegetated crater slope in this period. Wood macrocharcoals were however sporadically detected in three samples between 20,830-21,930 cal yr BP (1352, 1375, 1430 cm) suggesting that trees or shrubs were likely ocassionally sporadically present in the crater in this period of the LGM. Tree/shrub wood macrocharcoal remains and plant macrofossils were continuously detected in the sediment from ~15,700 cal yr BP (1092 cm) suggesting the expansion of trees and shrubs on the crater slope from this time onwards. *Betula nana* and *B. pubescens* were first recorded at 15,150 cal yr BP, followed by recoveries of *Pinus sylvestris* needles at 14,700 cal yr BP, i.e. directly at the onset of the lateglacial interstadial, when *Pinus* pollen accumulation rates also increased rapidly (Figure 6). In addition, *Larix decidua* needles were recently found in in the late glacial section of the SZA-2013 core of Lake St Anne at 1041 cm (~12,870 cal yr BP) overall suggesting that following an initial shrub and forest tundra phase characterised by *Betula pubescens* and *B. nana* around 15,700-15,100 cal yr BP, boreal forest elements expanded on the carter slope during the late glacial.

4.5. PCA, biome reconstruction and pollen compositional change analyses

The PCA biplot (Figure 7) separates clearly the Holocene pollen assemblages from the glacial assemblages along axis 1. Samples with high positive values along this axis are associated with temperate deciduous trees and *Picea abies*. The largest compositional change in the pollen spectra appears at ca. 11,600 cal yr BP (between 1027-1023 cm). Axis 2 separates GS-3, GS-2 and GI-1 (late glacial) pollen assemblages; negative values along this axis are associated with Poaceae, *Juniperus*, Cyperaceae, Caryophyllaceae and *Thalictrum*, while positive values with *Pinus*, *Betula* and *Artemisia*. The stratigraphic plot of Axis 2 sample scores suggest that the second largest compositional change is the pollen assemblages is at ~16,300 cal yr BP (between 1103-1107 cm).

The cumulative plot of plant types on Figure 3 shows that grassland and dry shrubland were the most abundant during the LGM, conifer trees representing mainly eurithermic pine forests also attained relatively high percentages (up to 60%); this plant type is however likely overrepresented due to low overall pollen accumulation rates and high pollen production of *Pinus*. Pollen compositional change (DCCA axis 1) is displayed on Figure 8. This curve indicates rapid compositional change at 23,000 and 21,000 cal yr BP, but otherwise the LGM pollen assemblages are rather stable. Similarly to the PCA results, pollen compositional change increase at 16,300, 14,700 and 12,700 cal yr BP. The largest compositional turnover (1.2 SD units) is between 12,700 and 11,000 cal yr BP.

5. **Discussion**

5.1. Physical environment during the LGM and last deglaciation

The frequent occurrence of coarse sand and gravel in the GS-3 and GS-2.1c sediment section of Lake St Anne can best be explained by ice floe transport and is thus interpreted as ice rafted debris (IRD) that in turn imply much longer ice-cover on the lake and unstable/sparsely vegetated crater slopes. IRD accumulation stops at 16,100 cal yr BP (Figures 3 and 8, Supplementary Table 2) suggesting that the crater slopes started to stabilize at this time and winter ice cover likely became shorter.

Frequent and abrupt fluctuation in Fe can reflect several different processes (redox changes, alternating input of terrigenous material, soil changes); Fe compounds furthermore can move in the sediment pore water, making the interpretation of the Fe peaks difficult. In order to disentangle these processes, we plotted Fe on the sediment photo for a short LG section of the core, where the most abrupt changes in Fe were found (Supplementary Figure 1). It is apparent that Fe shows increases either before or after major changes in sediment composition suggesting that post-depositional iron mobilisation is a likely cause of the iron increases during the late glacial and early Holocene. The dark humic horizons of turbidites also show Fe peaks occasionally in the LGM sediment layers, suggesting terrestrial inwash likely in association with FeS formation during highly reducing conditions (Kylander et al., 2011). Overall, the Fe and Fe/Ti curves suggest that the most frequent redox changes occurred during the late glacial likely in association with abrupt lake-level changes in this period. Low organic content associated with relatively high Si/Ti (an indirect measure of biogenic silica production and aeolian quartz; Liu et al., 2013) and Fe/Ti values during the LGM furthermore suggest that the lake was iron-rich, well-oxygenated and the generally low in-lake productivity was likely accompanied by relatively high aeolian silt input and/or increased diatom productivity until 20,000 cal yr BP, followed by strong fluctuation likely reflecting changes in diatom productivity (Figure 3). The lake internal plysicochemical environment (ie. oxygenated water bottom) likely facilitated the decomposition of organic matter during the LGM (e.g., Veres et al., 2009).

High and strongly fluctuating MS values during the LGM likely reflect the interplay between lake-internal chemical processes and aeolian input into the basin, and at varying intensity. Since the MS curve, a measure of the magnetic mineral concentration into the sediment, does not show strong correlation with the Fe and Fe/Ti ratio curves, and with the typically clastic element readings (e.g. Ti), we infer that an aeolian imprint is the most likely interpretation of the MS record over the LGM. Aeolian deposits (typical loess and loess-derived sediments) cover the lowlands surrounding the Ciomadul volcano, in places with deposits several meters thick. Grain-size analyses indicate that over this interval silt is the dominant particle size in Lake St Anne sedimentary sequence (Supplementary Figure 2); we thus infer intensive aeolian activity in the East Carpathians between 26,000-20,200 cal yr BP. Extremely high accumulation rates for aeolian deposits during this time interval have recently been inferred in a study of loess deposits, south of the Carpathians (Fitzsimmons and Hambach, 2014), corroborating our findings. Our data shows also good correspondence with the accumulation of thick loess deposits during the LGM in several lowland areas south, west and east of the Romanian Carpathians (Marković et al., 2008; Újvári et al., 2010; Novothny et al., 2011; Stevens et al., 2011).

Several periods of likely diminished aeolian input are also noticeable; the most conspicuous minima are between 22,000-21,000 and 23,500-23,000 cal yr BP (Figure 8). The first corresponds with increased arboreal pollen (AP%) suggesting increased regional woody cover at that time, while the second does not show concurrent arboreal pollen increase; *Pinus* pollen frequencies increase only after the low MS interval (Figure 8). However the 23,500-23,000 cal yr BP low MS interval is coincident with Greenland interstadias GI-2.1 and GI-2.2 (Rasmussen et al., 2014).

The XRF data suggest that clastic input into the lake decreased in several steps from ca. 16,500 cal yr BP (Figure 3). Although the timescale of the late glacial sediment section is ambiguous, major decrease in clastic input, as indicated by the Ti counts, occurred at ~16,200, 14,700, 12,500 cal yr BP. The timing of these decreases agrees well with the timing of significant and stepwise AP increases (mainly attributable to *Pinus* in the first two cases), the timing of major pollen compositional changes, organic content increases and changes in the green algae community of the lake (Figures 4, 5 and 8). The S and Ca peak between 16,200-15,000 cal yr BP coincides with the first phase of clastic input decrease and likely denotes a phase with intensive organic production, decomposition and accumulation of Ca and S compounds under fluctuating redox conditions at the core location. Increasing nutrient availability in the lake and rapidly changing environmental conditions are also corroborated by the green algae record (*Pediastrum*, *Scenedesmus* increases, Figure 5). The onset of the late glacial interstadial (GI-1e, around 14,700 cal yr BP) is well-marked in the element and LOI records. It shows a large increase in organic content, decreases in S and Ca that together with the sudden disappearance of green algae reflect warming, terrestrial productivity increase, lake level decrease and catchment soil stabilization. These proxy data suggest that the rapid warming at the onset of the late glacial interstadial (GI-1e) led to the seasonal desiccation of the lake at the core location, followed by water level increase at ca 13,200 cal yr BP when green algae re-appeared. Clastic input increased once again during GS-1, when Ti increased, organic content decreased. The timing of this event however precedes GS-1 in Greenland (Blockley et al., 2012), as we discussed in the chronology section, this is likely due to the bias of the age-depth model. The LOI and XRF data suggest that organic production increased steeply during the early Holocene, and the lake transformed into a peatbog with >90% organic accumulation (Magyari et al., 2009)

5.2. Pollen and plant macrofossil inferred vegetation changes and regional fire history

Our centennial-resolution pollen record shows three distinct vegetation phases within the last glacial maximum (26,000 – 19,000 cal yr BP; Clark et al., 2009) and clear vegetation responses to two short-term climatic fluctuations within this period (GI-2.1 and GI-2.2; Figure 8).

Qualitative and quantitative assessment (Figures 4 and 6) of the LGM pollen spectra from Lake St Anne suggests that between c. 26,350-22,870 cal yr BP the regional vegetation was composed of boreal forest steppe vegetation mainly with *Pinus* and *Larix*, *Juniperus* shrubs, grass steppes, shrubby tundra and steppe-tundra. A comparison with surface pollen samples from South Siberia suggested that the LGM ecosystems showed only weak similarity with the modern continental hemiboreal and taiga forests and forest steppes of South Siberia (Magyari et al., 2014). This comparison furthermore showed that despite the relatively high AP values (av. 42%), if statistically significant analogue vegetation was found, it was dry steppe and wet/mesic grassland (Magyari et al., 2014). Thus we infer that arboreal pollen percentages overestimate the actual share of trees in the LGM vegetation, explained by the large pollen production of pines (mainly *Pinus sylvestris*) (Seppä and Hicks, 2006). Another important woody component of the LGM flora was *Juniperus* (8-20%). This shrub is a common constituent of the LGM pollen assemblages in Europe (Tzedakis, 1999; Digerfeldt et al., 2000; Fletcher et al., 2010), but particularly high values are attained in some alpine GS-2.1a and late glacial (GI-1) pollen diagrams (e.g. Amman, 2000; Vescovi et al., 2007). Based on the modern ecology of *Juniperus* in the high mountains of Central Asia (Agakhanyants, 1981), we assume that *Juniperus* was mainly occupying northern slopes in the Carpathians where available moisture allowed replacement of meadow-steppe or steppe-tundra by *Juniperus* scrubland. Terrestrial plant macrofossils were not found in the LGM section of the sediment, only one conifer stomata and a few unidentified wood macrocharcoals at 20,830 and 21,930 cal yr BP (Table 3) suggesting that trees were likely not growing on the crater slopes. We assume that the diverse mixture of alpine tundra and steppe plants, and ruderal elements at least partially derived from the crater slopes (see Table 2 for herb flora composition). Aquatic plants were very rare in this period that is difficult to interpret, since we are still very close to the formation of the lake in this period following the last volcanic activity (Harangi et al., 2010; Karátson et al., 2013). The lake was nutrient poor and likely shallow in this phase.

A significant change in the vegetation composition was detected at 22,870 cal yr BP, when decreased representation of xerophytic herbs (*Artemisia* and *Chenopodim*-type) and increased representation of Poaceae and *Pinus* suggested regionally increasing woody cover associated with the expansion of grass-dominated steppe or steppe-tundra vegetation. The diversity of herbs further increased in this period, the start of which coincides with the GI-2.2 interstadial (Figures 4, 7; Rasmussen et al., 2014), while the end of it, 19,150 cal yr BP, corresponds with the end of the global last glacial maximum according to Clark et al. (2009). This phase of the LGM showed the highest palynological richness (Figure 4, Table 2) suggesting that the LGM herb flora of the East Carpathians was particularly well-developed and included tall forbs, steppe, tundra and talus slope elements (e.g. *Saxifraga hirculus*-type, *Saxifraga* sp., *Ranunculus*, *Aconitum*, Cariophyllaceae, *Thalictrum*, *Hypericum*). Polypodiaceae spores were also typically encountered in this phase, and the ferns that belong to this large group were likely associated with the boreal ecosystems of lower altitude in this period. Other important characteristics of this final LGM period were the increased regional fire frequencies as suggested by the microcharcoal accumulation rates and the increased representation of temperate deciduous pollen types (*Corylus*, *Fagus*, *Ulmus*, *Carpinus betulus*, *Fraxinus excelsior*- type and *Quercus*). Increased regional fire events suggest that the climate was strongly continental and combustible biomass was regionally available (Daniau et al., 2010). We also infer that the presence of temperate deciduous tree pollen supports population genetic inferences (Palmé and Vendramin, 2002; Heuertz et al., 2004; Magri et al., 2006), according to which some temperate deciduous tree species (e.g. *Fagus sylvatica*, *Fraxinus excelsior*, *Corylus avellana*) were likely present sporadically at lower altitudes in the western, rainward slopes of the Carpathians or in the adjoining lowlands. The possible LGM survival of temperate deciduous trees in the Carpathian Basin and adjoining mountain area has been discussed recently by Magyari et al. (2014). Comparing three LGM pollen sequences from this region (one is Lake St Anne) this study concluded that both LGM climate model and reconstructed climatic parameters would allow for the survival of temperate deciduous trees especially in this region; pollen data support their restricted occurrence, but macrofossils dating to the LGM have yet to confirm their local presence. Macrofossils of temperate deciduous trees dated to the LGM are yet missing, but appear as north as the Moravian basin during MIS3 (Willis and van Andel, 2004). The St Anne pollen diagram shows repeated occurrence and occasionally increased percentages of temperate deciduous pollen types (esp. *Quercus*, *Corylus*, *Fraxinus excelsior*-type, *Ulmus*, *Fagus*, *Carpinus betulus*) that is provoking, since most S European pollen records show similar or even lower values, and the recorded values in the Lake St Anne pollen diagram are particularly prominent for *Fagus* (Figure 4, Supplementary Figure 3; Tzedakis et al., 2002, 2004, 2013; Allen et al., 1999; Müller et al., 2011). Even though the Tusnad Gorge (630 m a.s.l.) and Ciuc Basin (640-700 m a.s.l.) are characterised by strengthened continental climate due to basin effect (absolute minimum-38 ^{o}C, absolute maximum 33 ^{o}C; annual temperature 3.8-7.6 ^{o}C; Ujvárosi et al., 1995; Demeter and Hartel, 2007), there are several hills with warm microclimate that support today warm-indicator flora (e.g. *Prunus nana, Salvia nutans, Spiraea crenata*, *Hiacinthella leucophyllea*) lying south and west of Lake St Anne (e.g. Vargyas Valley (555-945 m), Perkő near Sânzieni (588-720 m), the Olt river valley near Ariușd (500 m); see Jakab et al., 2007). If temperate trees survived the LGM in the nearby lower mountains, then these areas within the elevation range 500-600 m a.s.l. were likely the most suitable habitats for temperate tree growth. The increased abundance of wet-tundra vegetation in this period is best captured by the *Saxifraga hirculus*-type pollen curve that attains the highest values in this phase (22,870-19,150 cal yr BP, Figure 8). Overall, our data suggest that the LGM was less arid in the East Carpathian Mountains than in the SE Mediterranean Basin and Thrace (Tzedakis et al., 2004; Müller et al., 2011; Connor et al., 2013), while Ioannina in NW Greece was likely comparably humid but considerably warmer (especially in winter) allowing for larger populations of temperate deciduous trees (Tzedakis et al., 2002). On the other hand, the Lake St Anne pollen record suggests that if temperate deciduous trees survived the LGM in the region, they might have been disfavoured by available moisture decrease and xerophytic steppe expansion after the LGM, between 19,000 – 15,000 cal yr BP, which period showed the expansion of *Artemisia*, *Chenopodium*-type and several other elements of xerophitic steppes in the area of Lake St Anne (SZA-3, Figures 3, 4 and 7). Alpine and tundra plants were still present in this period (e.g. *Polygonum viviparum*, *Dryas octopetala*). We infer an increase in overall vegetation cover from increasing PAR values; decreasing forest fire activity, and a major increase in boreal woodland cover (*Betula*, *Pinus*, *Larix* and *Picea*) from ~16,300 cal yr BP. According to the preliminary plant macrofossil record, trees and shrubs likely appeared on the crater slope a few hundered years later, around 15,700 cal yr BP, when several unidentified wood macrochrcoals were found in the sediment. Subsequently, *Betula nana* and *B*. *pubescens* appeared at 15,150 cal yr BP, followed by the first recovery of *Pinus sylvestris* at 14,700 cal yr BP (Table 3). These findings corroborate the pollen based inference that the crater slope became partially wooded already prior to the onset of the late glacial interstadial (GI-1), and elements of shrub/forest tundra and boreal forest associations were present on the crater slope suggesting the emergence of boreal ecosystems similar to the present vegetation of S Siberia (Chytrý et al., 2008; Magyari et al., 2014). From 16,300 cal yr BP green algae relative frequencies (*Pediastrum*, *Scenedesmus*) and aquatic macrophytes (*Myriophyllum verticillatum*) indicated increasing nutrient availability and likely increasing lake level, although this inference may contradict with the xerophytic steppe expansion. From the overall vegetation cover increase we assume that *Artemisia* and *Chenopodium*-type dominated steppe likely expanded on places that were formerly either not vegetated or covered by *Juniperus*, which declined in this period. Increasing pollen percentages and accumulation rates of *Betula*, *Pinus*, *Larix*, *Picea* and *Ulmus* suggest that available moisture increased with temperature after 16,300 cal yr BP. The short-term re-increase of *Juniperus* and Poaceae around 17,000 cal yr BP can likely be connected to cooling during Heinrich stadial 1 (within GS-2.1a; Figures 4 and 7).

The final pollen zone of the last glaciation covers the late glacial (GI-1 and GS-1). Due to very low sediment accumulation rates in this period, the pollen diagram is not very detailed. The onset of the late glacial interstadial (GI-1e) is marked by abrupt increase in *Pinus* pollen percenatges and PAR, and more gradual increases in *Picea abies*, *Larix*, *Betula* and a major drop in *Juniperus* pollen values indicating afforestation by boreal trees mainly. Pine-birch (*Pinus sylvestris* - *Betula pubescens*) and larch (*Larix decidua*) forests likely expanded in the vicinity of Lake St Anne as indicated by the presence of their macrofossils (Table 3), but notably temperate deciduous tree pollen frequencies remained lower in this period than between 22,870 and 19,150 cal yr BP. This can at least partially be explained by the massive expansion of the rich pollen producer *Pinus sylvestris* during the late glacial (see *Pinus* PAR values on Figure 6). Decreasing AP values and re-expansion of *Artemisia* and *Chenopodium*-type between 1047 and 1035 cm (13,300-12,300 cal yr BP) mark the GS-1 stadial. An important feature of the aquatic pollen assemblages is the disappearance or decrease of green algae that together with the organic content increase suggest decreasing lake level during the late glacial interstadial (GI-1). *Scenedesmus* and *Pediastrum* relative frequencies, on the other hand increased during GS-1 suggesting increasing nutrient availability and possibly increased lake levels (probably due decreased evaporation or decreased tree cover on the crater slope). From these data we may infer that in the East Carpathian Mountains cooling during the LGM and late glacial did not necessarily coincide with decreasing lake levels; temperature decrease likely compensated at least partially for the decreasing rainfall via decreased evaporation. A similar relationship has been found in Serbian last glacial loess sequences by Zech et al. (2013). In this continental and considerably warmer lowland area, lipid biomarker studies suggested increasing woody cover during stadial phases and increasing steppe cover during the warm interstadials, overall pointing to decreasing moisture availability during the warm interstadials.

The above detailed vegetation picture agrees well with continent-wide LGM vegetation assessment of Fletcher et al. (2010), which showed decreasing severity of stadial conditions in Eastern Europe, explained by the larger distance of this area to the North Atlantic.

5.3. Distinctive features of the GS-2 and GS-3 vegetation in comparison with more southerly latitudes and westerly longitudes in Europe

When the LGM pollen spectra of Lake St Anne are compared with the relevant sections (26-19 ka cal yr BP) of several long SE European pollen records (mainly the Eastern Mediterranean basin), Lake St Anne stands out by having 1) generally higher AP frequencies during the LGM due higher representation of *Pinus* and *Juniperus*; 2) comparable and in some cases even higher representation of temperate deciduous pollen types; 3) an expansion of xerophitic steppe vegetation after the LGM (at c. 19 ka cal yr BP) that is antagonistic with the decreasing share of xerophitic steppes in several SE european mountains at the same time (Allen et al., 1999; Tzedakis, 2002; Panagiotopolous et al., 2013). Similar to the E Carpathians, steppe expansion in the Iberian Penninsula also commenced after the global LGM; however, it occurred later, and was clearly associated with Heinrich stadial 1 (around 17,500 cal yr BP). Moreno et al. (2012) explained the dry conditions with a considerable reduction in the Atlantic Meridional Overturning Circulation (AMOC) that initiated sea ice formation and reduced sea surface evaporation in the North Atlantic region. Contrary to this, the major vegetation change at Lake St Anne during Heinrich stadial 1 was the recurrent expansion of *Juniperus* (against *Pinus*; Figures 4 and 8) and the decrease of xerophytic steppe elements suggesting that the vegetation likely responded to cooling forcing.

In several south Europen long pollen records, short term AP increases are coincident with $\delta^{18}O$ maxima in Greenland during MIS 3 (Allen et al., 1999, 2000; Tzedakis et al., 2002; Panagiotopoulos et al., 2013; Müller et al., 2011). However, MIS 2 (broadly corresponding to GS-3, GS-2 and GS-4) is characterised by steadily low AP values in these records (Tzedakis et al., 2013; Helmes et al., 2014), even though weak stadial/interstadial fluctuations are still observebale in the Greenland isotope records (Figure 8). It is therefore not surprising that the *Pinus* percentage and MS fluctuations in core SZA-2010 cannot be strictly connected to stadial/interstadial fluctuation within the GS-2 and GS-3 section of Lake St Anne (Figure 8; Rasmussen et al., 2014).

Due to the calcareous or volcanic settings, chronologies of the LGM and lateglacial sections of several SE European long cores are loaded with similar uncertainties/biases like Lake St Anne (Allen et al., 1999; Digerfeldt et al., 2000; Tzedakis, 2002; Jones et al., 2013). Bearing in mind possible age offsets, an important feature of these records is the early start of afforestation by conifers and/or temperate deciduous trees after the LGM. In most records significant increases of arboreal pollen start at 17,000 – 16,000 cal yr BP (Tinner et al., 1999; Müller et al., 2011; Magyari et al., 2014), similarly to Lake St Anne. In this context, the onset of the late glacial interstadial (GI-1) is marked by secondary rises in arboreal pollen, suggesting that 1) afforestation of both lowland and mid mountain habitats commenced gradually after and/or during Heinrich stadial 1 (GS-2.1a), and similarly to the Carpathians, SE European lowlands and mid mountains were at least partially wooded by this time.

Melt-water pulses in the Black Sea region were demonstrated by a depletion of $\delta^{18}O$ values in isotope records of stalagmite So-1 from the Sofular Cave and from the combined Black Sea $\delta^{18}O$ record (Figure 8; Fleitmann et al., 2009; Badertscher et al., 2011) at ~16.1 ka BP, which date shows good correspondence with the earliest onset of *Pinus* PAR increase and wood macrocharcoal/macrofossil expansion in the Lake St Anne proxy record and reinforces the origin of available moisture increase already at 16.1 ka (Fleitmann et al., 2009). Note however that despite the inevitable sediment source changes in the Black Sea (red layer deposition suggesting water level increase and connection with the Caspian Sea) arboreal vegetation in the Black Sea area did not increase until 14,500 cal yr BP, except for a slight increase in temperate deciduous biome scores from 15,400 cal yr BP (Shumilovskikh et al., 2012). In the Bulgarian Thracian Plain, available pollen data suggest the persistence of steppic conditions from the LGM to the late glacial (Connor et al., 2013); here the composition of the vegetation shows a major change from cold steppe to semi-desert at 17,900 cal yr BP supporting the notion of intensifying summer drought in this region.

Overall, this comparison suggest that vegetation in the East Carpathians responded to warming and increasing moisture more rapidly via the spread of shrub tundra, forest tundra, boreal and cool temperate trees during the last deglaciation, while the Black Sea zone still remained dominated by various steppe biomes (Shumilovskikh et al., 2012; Connor et al., 2013).

Climate modelling experiments (e.g. Strandberg et al., 2011; Huntley et al., 2013) suggest a shift of the summer westerly jet from the Mediterranean Sea region to a more northerly position between 18,000 and 12,000 cal yr BP, in response to the decrease in ice volume. Summer insolation was increasing at the same time (Berger and Loutre, 1991), and our proxy data suggest that the cumulative ecosystem impact of these climatic changes was twofold in the East Carpathians: an increase in warm steppes between 19-16.1 ka reflecting the overwhelming effect of summer isolation increase in this period, followed by the joint effect of warming and precipitation increase around 16,100 cal yr BP.

5.4. Comparison with late glacial (GI-1, GS-1) pollen, plant macrofossil and stable isotope profiles in the Romanian Carpathians

Although the late glacial section of core SZA-2010 has low sampling resolution, and deposition times are low (70-124 yr cm^{-1}), several similarities can be identified when the pollen and plant macrofossil records are compared with the relatively large network of late glacial sites in the Romanain Carpathians (Feurdean et al., 2007, 2012). In the vicinity of Lake St Anne, the Luci and Mohoş peat bog pollen profiles cover the late glacial (Tanţău et al., 2003, 2014), and similarly to SZA-2010 show large increase in *Pinus* pollen frequencies at the beginning of GI-1e (Figure 8), around 14,700 cal yr BP (Feurdean et al., 2007, 2012, 2014; Tanţău et al., 2014). None of these sequences show high *Juniperus* pollen frequencies in their bottom layers comparable to pollen zones SZA-1 to SZA-3 (Table 2), but *Juniperus* pollen is continuously present at values 1-5% until 14,700 cal yr BP overall suggesting that most of the pollen sequences do not extend beyond 17,000 cal yr BP and hence do not cover Heinrich stadial 1. The longest pollen sequence, Avrig (400 m a.s.l.) extends back to ~19,000 cal yr BP according to its updated age-depth model (Feurdean et al., 2014). Low *Juniperus* values in the lower part of this core suggest that *Juniperus* shrubs were more abundant at higher altitudes in the mountains during the terminal part of GS-2, while at low altitudes *Pinus* and mixed steppe components played a more important role. Notable is that both the Setregoiu and Avrig pollen sequences show the first increase of *Pinus* pollen frequencies around 16,000 cal yr BP, corroborating that *Pinus* expanded in both low and mid altitudes before the onset of GI-1.

Regarding the macrofossil detected first occurrence times of various trees in the Romanian Carpathians the Stergoiu (790 m a.s.l.) and Preluca Tiganului (730 m a.s.l.) sequences show good agreement with Lake St Anne regarding the on-site arrival time of *Pinus sylvestris* (14,500 cal yr BP at Steregoiu; Feurdean et al., 2012). These two mid altitude sites however showed a much more diverse wood macrofossil assemblage (*Populus*, *Alnus*, *Picea*, *Larix*, *Prunus padus*, *Pinus cembra*, *Betula pubescens*, B. *pendula*, *P*. *mugo*, *P*. *sylvestris*, *Salix*) during the late glacial suggesting that climate was likely more favourable for open forest development at lower altitudes. Notable is that *Betula pubescens* and *B*. *nana* were already recorded in core SZA-2010 before the onset of GI-1.

When we compare the palynological richness inferred plant diversity changes in various parts of the Romanian Carpathians during the terminal part of GS-2, during GI-1 and GS-1, we see that at Lake St Anne plant diversity likely significantly decreased during GI-1 relative to GS-2 (including the LGM). Average palynological richness values dropped from 25-21 to 17 (Figure 4 and Table 2), the latter being similar to late glacial interstadial values at other sites (Feurdean et al., 2012). This is likely attributable to the extirpation of various alpine and tundra herbs in the pollen source area of Lake St Anne at the onset of GI-1. Note however that due to the increasing vegetation cover of the study area in GI-1, it is also conceivable that the effective pollen source area of the lake has changed in this period that might bias the inferred plant diversity changes (van der Knaap, 2009). Nonetheless, other pollen records in the Romanian Carpathians show comparable palynological richness values (10-25) during GI-1 and GS-2 with the strongest increases at the onset of the Holocene explained by recruitment much exceeding local extirpation. Palynological richness also increases temporarily in the Early Holocene in the Lake St Anne record, but here the amplitude of this increase is not the largest in the record (Figure 4). Another important and so far unique characteristic of the SZA-2010 pollen record is the repeated decrease of palynological richness at the onset of each pollen zone implying that the first step of each climate induced vegetation reorganization was a decrease in plant diversity followed by steep increases. The large compositional turnover (1.2 SD units on Figure 8) of the vegetation between 12,700 and 11,000 cal yr BP compares well with other Romanain pollen profiles (Feurdean et al., 2012) and confirms that similarly to other mid altitude sites in the Romanian Carpathians the largest floristic compositional change occurred between GS-1 and the Holocene.

Stable isotope records of several late glacial stalagmites in the Romanian Carpathians (Tămaş et al., 2005; Constantin et al., 2007) suggest that at the onset of each late glacial warming phase moisture availability (inferred by $\delta^{13}C$) also increased, which inference was also supported by the pollen and plant macrofossil based climatic inferences (Feurdean et al., 2008, 2012). As discussed above, the Lake St Anne pollen and plant macrofossil records agree well with other Romanian records, therefore the terrestrial vegetation components seemingly support the stable isotope and other pollen based inferences. However, planktonic green algae in Lake St Anne are in partial disagreement with this climatic interpretation. This record shows that following an initial increase in both diversity and relative frequancies of green algae from ~16,300 cal yr BP (see Sum *Pediastrum* and *Scenedesmus* on Figure 5), an abrupt decrease can be detected at ~14,600 cal yr BP suggesting that planktonic habitats and thus likely water level decreased at the onset of the late glacial interstadial (GI-1). Even more surprisingly, relative frequencies of planktonic green algae increased again at ~13,300 cal yr BP when xerophitic steppe herbs were on increase (e.g. *Artemisia*, Chenopodiaceae) and overall hinted at the onset of GS-1. Therefore this record infers that lake level and thus likely effective moisture (precipitation minus actual evapotranspiration) migh have decreased with warming. This feature of the Lake St Anne paleorecord agrees with some lipid-based inferences of the Serbian loess sequences (Zech et al., 2013); however, it needs further testing by the diatom study of the same deposit before any firm conclusion is made. We also need to understand why a mismatch between the $\delta^{13}C$ stalagmite and green algae records exist. Is it possible that the difference arises because $\delta^{13}C$ in stalagmites reflects annual moisture changes, while green algae indicate summer water-depth changes? Alternatively, can increasing woody cover on the crater slope decrease runoff in the warm intervals and thereby decrease water-depth?

6. Conclusions

Pollen based reconstruction of the LGM vegetation types provided evidence for attenuated response of the regional vegetation to maximum global cooling. Between ~22,870 and 19,150 cal yr BP we found species rich steppe-tundra and grass steppe vegetation at mid altitudes (~1000 m a.s.l.) in the mountain in association with *Juniperus* shrubland; furthermore, our data supported earlier inferences for the persistence of coniferous and deciduous trees likely in parkland forests at lower altitudes (with *Pinus*, *Betula*, *Salix and Picea*). Our pollen record supports population genetic inferences regarding the possible regional survival of some temperate deciduous trees (*Fagus sylvatica*, Corylus *avellana*, *Fraxinus excelsior*) in this period. Probably the most intriguing result of this study is the increased regional biomass burning between 22,870- 19,150 cal yr BP that is antagonistic with the global trend of decreased biomass burning. Increased regional fire activity confirms the regional presence of combustible biomass and indicates extreme continentality in this period, likely with relatively warm and dry summers.

Xerophytic steppes expanded in the East Carpathian forelands from ~19,150 cal yr BP. Our pollen accumulation rate record suggested that this expansion took place partially at the expense of the grass steppes and boreal forest steppe. This vegetation change implies that warming directly after the LGM likely resulted in increasing summer drought in the East Carpathians and its forelands. We conclude that xerophytic steppe expansion is a characteristic feature of the East-Central European sector at latitudes 46-48 ^{o}N, as similar vegetation changes were also demonstrated in the Pannonian Basin.

In accordance with the Black Sea and Sofular cave proxy records, forest expansion in the E Carpathians started already around 16,300 cal yr BP. *Pinus* and *Betula* dominated forests expanded in accordance with available moisture increase in the southern Black Sea area, permafrost melting and wetland expansion in the European Russian Plain.

Acknowledgements

This paper is part of the PROLONG project supported by the OTKA Research Funds (PD73234, NF101362). EKM acknowledges the support of the Bolyai Scholarship (BO/00518/07), the Humboldt Fellowship, the Hungarian Academy of Sciences and the CRC 806 ("Our way to Europe"). D.V. acknowledges the support from project PN-II-ID-PCE-2012-4-0530 'Millennial-scale geochemical records of anthropogenic impact and natural climate change in the Romanian Carpathians'. This is MTA–MTM Paleo Contribution No. 194. We would like to thank the help of István Papp and the Lacul Sfânta Ana & Mohoş Nature Reserve administration during the drilling operations.

References

Agakhanyants, O.Ye. (1981) Aridnye gory SSSR (Arid Mountains of the USSR). Moscow, Mysl, 270 p. (in Russian).

Allen, J.R.M., Brandt, U., Brauer, A., Hubberten, H.W., Huntley, B. (1999) Rapid environmental changes in southern Europe during the last glacial period, Nature 400: 740-743.

Allen, J.R.M., Watts, W.A., Huntley, B. (2000) Weichselian palynostratigraphy, palaeovegetation and palaeoenvironment; the record from Lago Grande di Monticchio, southern Italy, Quaternary International 73(4): 91-110.

Ammann, B. (2000) Biotic responses to rapid climatic changes: Introduction to a multidisciplinary study of the Younger Dryas and minor oscillations on an altitudinal transect in the Swiss Alps. Palaeogeography, Palaeoclimatology, Palaeoecology 159:191-201.

Andersen, K. K., Azuma, N., Barnola, J. M., Bigler, M., Biscaye, P., Caillon, N., Chappellaz, J., Clausen, H. B., DahlJensen, D., Fischer, H., Fluckiger, J., Fritzsche, D., Fujii, Y., Goto-Azuma, K., Gronvold, K., Gundestrup, N. S., Hansson, M., Huber, C., Hvidberg, C. S., Johnsen, S. J., Jonsell, U., Jouzel, J., Kipfstuhl, S., Landais, A., Leuenberger, M., Lorrain, R., Masson-Delmotte, V., Miller, H., Motoyama, H., Narita, H., Popp, T., Rasmussen, S. O., Raynaud, D., Rothlisberger, R., Ruth, U., Samyn, D., Schwander, J., Shoji, H., Siggard-Andersen, M. L., Steffensen, J. P., Stocker, T., Sveinbjornsdottir, A. E., Svensson, A., Takata, M., Tison, J. L., Thorsteinsson, T., Watanabe, O., Wilhelms, F., White, J. W. C., and Project, N. G. I. C. (2004) High-resolution record of Northern Hemisphere climate extending into the last interglacial period. Nature 431: 147–151.

Badertscher, S., Fleitmann, D., Cheng, H., Edwards, R. L., Gokturk, O. M., Zumbuhl, A., Leuenberger, M. and Tuysuz, O. (2011) Pleistocene water intrusions from the Mediterranean and Caspian Seas into the Black Sea. Nature Geoscience 4 (4): 236-239.

Bálint, M., Ujvárosi, L., Theissinger, K., Lehrian, S., Mészáros, N. & Pauls, S. (2011) The Carpathians as a major diversity hotspot in Europe. In: Zachos, F. & Habel, J. (eds) Biodiversity Hotspots, pp. 189–205, Springer, Heidelberg, Germany.

Bennett, K. D. (2007) Psimpoll. http://www.chrono.qub.ac.uk/psimpoll/psimpoll_manual/4.27/psimpoll.htm (last accessed on 10 Feb 2014)

Bennett, K.D., Willis, K.J. (2002) Pollen. In: J.P. Smol, H.J. B. Birks, W.M. Last (eds) Tracking Environmental Change Using Lake Sediments, Volume 3: Terrestrial, Algal, and Siliceous Indicators. Kluwer Academic Publishers, Dordrecht, The Netherlands, pp. 5-32.

Berger, A., Loutre, M-F. (1991) Insolation values for the climate of the last 10 million of years. Quaternary Science Reviews 10(4): 297-317.

Beug, H. J. (2004) Leitfaden der Pollenbestimmung für Mitteleuropa und angrenzende Gebiete. Verlag Dr. Friedrich Pfeil, München.

Birks, H.J.B. (2007) Estimating the amount of compositional change in late-Quaternary pollen stratigraphical data. Vegetation History and Archaeobotany 16: 197–202.

Birks, H.J.B., Birks, H.H. (2008) Biological responses to rapid climate change at the Younger Dryas–Holocene transition – succession, diversity, turnover, and rates of change. The Holocene 18: 19-30.

Birks, J.B. , Willis, K.J.(2008) Alpines, trees, and refugia in Europe. Plant Ecology and Diversity 1: 147–160.

Blaauw, M., Christén, A. (2013) Bacon manual – v2.2. http://chrono.qub.ac.uk/blaauw/manualBacon_2.2.pdf (last accessed on 10 Feb 2014)

Blockley, S. P. E., Lane, C. S., Hardiman, M., Rasmussen, S. O., Seierstad, I. K., Steffensen, J. P., Svensson, A., Lotter, A. F., Turney, C. S. M. & Ramsey, C. B. (2012) Synchronisation of palaeoenvironmental records over the last 60,000 years, and an extended INTIMATE event stratigraphy to 48,000 b2k. Quaternary Science Reviews 36: 2-10.

Blunier, T., Spahni, R., Barnola, J.-M., Chappellaz, J., Loulergue, L., Schwander, J. (2007) Synchronization of ice core records via atmospheric gases. Climate of the Past 3(2): 325-330.

Chytrý, M., Danihelka, J., Kubešová, S., Lustyk, P., Ermakov, N., Hájek, M., Hájková, P., Kočí, M., Otýpková, Z., Roleček, J., Řezníčková, M., Šmarda, P., Valachovič, M., Popov, D., Pišút, I. (2008) Diversity of forest vegetation across a strong gradient of climatic continentality: Western Sayan Mountains, southern Siberia. Plant Ecology 196: 61–83.

Clark, P.U., Dyke, A.S., Shakun, J.D., Carlson, A.E., Clark, J., Wohlfarth, B., Mitrovica, J.X., Hostetler, S.W., McCabe, A.M. (2009) The Last Glacial Maximum. Science 325(5941): 710-714.

Connor, S.E., Ross, S.A., Sobotkova, A., Herries, A.I.R., Mooney, S.D., Longford, C., Iliev, I. (2013) Environmental conditions in the SE Balkans since the Last Glacial Maximum and their influence on the spread of agriculture into Europe. Quaternary Science Reviews 68: 200-215.

Constantin, S., Bojar, A.V., Lauritzen, S.E. & Lundberg, J. (2007) Holocene and Late Pleistocene climate in the sub-Mediterranean continental environment: a speleothem record from Poleva Cave (Southern Carpathians, Romania). Palaeogeography, Palaeoclimatology, Palaeoecology, 243, 322–338.

Croudace, I. W., Rindby, A., Rothwell, R. G. (2006) ITRAX: description and evaluation of a new multi-function X-ray core scanner. Geological Society, London, Special Publications 267 (1): 51-63.

Daniau, A.L., Harrison, S.P., Bartlein, P.J. (2010) Fire regimes during th last glacial. Quaternary Science Reviews 29: 2918-2930.

Demeter L., Hartel, T. (2007) On the absence of the Agile Frog Rana dalmatina from the Ciuc basin. North-Western Journal of Zoology 3(1): 9-23.

Diaconu, D.C., Mailat, E. (2010) Complex study of the lacustrian ecosystems of Mohoş swamp. Lakes, reservoirs and ponds 4(1): 70-78. Romanian Limnogeographical Association.

Digerfeldt, G., Olsson, S., Sandgren, P. (2000) Reconstruction of lake-level changes in lake Xinias, central Greece, during the last 40 000 years. Palaeogeography, Palaeoclimatology, Palaeoecology 158: 65–82.

Drăguşin, V., Staubwasser, M., Hoffmann, D.L., Ersek, V., Onac, B.P., Veres, D. (2014) Constraining Holocene hydrological changes in the Carpathian-Balkan region using speleothem ^{18}O and pollen-based temperature reconstructions. Climate of the Past Discussion 10: 381–427.

Fábián, S. Á., Kovács, J., Varga, G., Sipos, G., Horváth, Z., Thamó-Bozsó, E. & Tóth, G. (2013) Distribution of relict permafrost features in the Pannonian Basin, Hungary. Boreas, *in press*.

Fărcaş, S., de Beaulieu, J.L., Reille, M., Coldea, G., Diaconeasa, B., Goeury, C., Goslar, T., Jull, T. (1999) First ^{14}C dating of Late Glacial and Holocene pollen sequences from the Romanian Carpathians. Comptes Rendues de l'Académie des Sciences de Paris, Sciences de la Vie 322: 799–807.

Fărcaş, S., Tanţău, I., Mîndrescu, M., Hurdu, B. (2013) Holocene vegetation history in the Maramureş Mountains (Northern Romanian Carpathians). Quaternary International 293: 92-104.

Fér, T., Vašák, P., Vojta, J., Marhold, K. (2007) Out of the Alps or the Carpathians? Origin of Central European populations of *Rosa pendulina*. Preslia 79: 367–376.

Feurdean, A., Bennike, O. (2004) Late Quaternary palaeoecological and palaeoclimatological reconstruction in the Gutaiului Mountains, NW Romania. Journal of Quaternary Science 19: 809–827.

Feurdean, A., Wohlfarth, B., Björkman, L., Tanţău, I., Bennike, O., Willis, K., Farcaş, S., Robertsson, A.M. (2007) The influence of refugial population on Lateglacial and early Holocene vegetational changes in Romania. Review of Palaeobotany and Palynology 145: 305–320.

Feurdean, A., Klotz, S, Brewer, S, Mosbrugger, V., Tămaş, T., Wohlfarth, B. (2008) Lateglacial climate development in NW Romania — Comparative results from three quantitative pollen-based methods. Palaeogeography, Palaeoclimatology, Palaeoecology 265: 121-133.

Feurdean, A., Tanţău, I., Fărcaş, S. (2011) Holocene variability in the range distribution and abundance of *Pinus*, *Picea abies*, and *Quercus* in Romania; implications for their current status. Quaternary Science Reviews 30: 3060-3075.

Feurdean, A., Tămaş, T., Tanţău, I., Fărcaş, S. (2012a) Elevational variation in regional vegetation responses to late-glacial climate changes in the Carpathians. Journal of Biogeography 39: 258–271.
Feurdean, A., Spessa, A., Magyari, E.K., Willis, K.J., Veres, D., Hickler, T. (2012b) Trends in biomass burning in the Carpathian region over the last 15,000 years. Quaternary Science Reviews 45: 111-125.
Feurdean, A., Parr, C.L., Tanţău,, I., Fărcaş, S., Marinova, E., Perşoiu, I. (2013a) Biodiversity variability across elevations in the Carpathians: parallel change with landscape openness and land use. The Holocene 23 (6): 869-881.
Feurdean, A., Bhagwat, S.A., Willis, K.J., Birks, H.J.B., Lischke, H., Hickler, T. (2013b) Tree Migration-Rates: Narrowing the Gap between Inferred Post-Glacial Rates and Projected Rates. PLoS ONE 8(8): e71797.
Feurdean, A., Persoiu, A., Tanţău, I., Stevens, T., Marković, S., Magyari, E.K., Onac, B.B., Andric, M., Connor, S., Galka, M., Hoek, W.Z., Lamentowicz, M., Sümegi, P., Persoiu, I., Kolaczek, P., Petr Kuneš, P., Marinova, E., Slowinski, M., Michczyńska, D., Stancikaite, M., Svensson, A., Veski, S., Fărcaş, S., Tămaş, T., Zernitskaya, V., Timar, A., Tonkov, S., Tóth, M; Willis, K.J., Płóciennik, M., Gaudenyi, T. (2014) Climate variability and associated vegetation response throughout Central and Eastern Europe (CEE) between 8 and 60 kyrs ago. Quaternary Science Reviews, 10.1016/j.quascirev.2014.06.003
Fitzsimmons, K.E., Hambach, U. (2014) Loess accumulation during the last glacial maximum: evidence from Urluia, southeastern Romania. Quaternary International. DOI:10.1016/j.quaint.2013.08.005
Fleitmann, D., Cheng, H., Badertscher, S., Edwards, R.L., Mudelsee, M., Gokturk, O.M., Fankhauser, A., Pickering, R., Raible, C.C., Matter, A., Kramers, J. and Tuysuz, O. (2009) Timing and climatic imprint of Greenland interstadials recorded in stalagmites from Northern Turkey. Geophysical Research Letters 36: L19707.
Fletcher, W.J., Sánchez Goñi, M.F., Allen, J.R.M., Cheddadi, R., Coumbourieu-Nebout, N., Huntley, B., Lawson, I.T., Londeix, L., Magri, D., Margari, V., Müller, U.C., Naughton, F., Novenko, E., Roucoux, K.H., and Tzedakis, P.C. (2010) Millennial-scale variability during the last glacial in vegetation records from Europe. Quaternary Science Reviews 29: 2839-2864.
Göktürk , O.M., Fleitmann, D., Badertscher, S., Cheng, H., Edwards, R.L., Leuenberger, M., Frankhauser, A., Tüysüz , O. and Kramers, J. (2011) Climate on the Southern Black Sea coast during the Holocene: implications from the Sofular Cave record. Quaternary Science Reviews 30 (19-20): 2433-2445.
Harangi, Sz, Molnár, M., Vinkler, A.P., Kiss, B., Jull, A.J.T., Leonard, A.E., (2010) Radiocarbon dating of the last volcanic eruptions of Ciomadul volcano, Southeast Carpathians, eastern–central Europe. Radiocarbon 52 (2–3): 1498–1507.
Helmens, K. F. (2014) The Last InterglacialeGlacial cycle (MIS 5e2) re-examined based on long proxy records from central and northern Europe. Quaternary Science Reviews 86: 115-143.
Heuertz, M., Fineschi, S., Anzidei, M., Pastorelli, R., Salvini, D., Paule, L., Frascaria-Lacoste, N., Hardy, O.J., Vekemans, X., Vendramin, G.G. (2004) Chloroplast DNA variation and postglacial recolonization of common ash (*Fraxinus excelsior* L.) in Europe. Molecular Ecology 13: 3437–3452.
Heyman, B.M., Heyman, J., Fickert, T., Harbor, J.M. (2013) Paleo-climate of the central European uplands during the last glacial maximum based on glacier mass-balance modeling. Quaternary Research 79: 49–54.
Huntley, B., Allen, J.R.M., Collingham, Y.C., Hickler, T., Lister, A.M., Singarayer, J., Stuart, A.J., Sykes, M.T., Valdes, P.J. (2013) Millennial climatic fluctuations are key to the structure of last glacial ecosystems. PLoS One 8 (4): e61963.
Jakab, G., Csergő, A., Ambrus, L. (2007) Adatok a Székelyföld (Románia) flórájának ismeretéhez I (New data to the flora of Szeklerland I. (Romania)). Flora Pannonica, Journal of Phytogeography & Taxonomy 5: 135-165. (in Hungarian with English summary).

Jakab, S., Füleky, G., Fehér, O. (2005) Soils of Eastern Carpathian mountains. Carpathi 13: 7-8. ISSN 1335-9908. Journal for Nature Conservation. Research, Monitoring & Management. In Carpathian Protected Areas, Bratislava.

Jakab, S. (2011) Andosols of the East Carpathian volcanic range. Acta Universitatis Sapientiae Agriculture and Environment 3: 110-121.

Jankovská, V., Pokorný, P. (2008) Forest vegetation of the last full-glacial period in the Western Carpathians (Slovakia and Czech Republic). Preslia 80: 307-324.

Jones, T.D., Lawson, I.T., Reed, J.M., Wilson, G.P., Leng, M.J., Gierga, M., Bernasconi, S.M., Tzedakis, P.C. (2013) Diatom-inferred late Pleistocene and Holocene palaeolimnological changes in the Ioannina basin, northwest Greece. Journal of Paleolimnology 49: 185-204.

Jost, A., Lunt, D., Kageyama, M., Abe-Ouchi, A., Peyron, O., Valdes, P.J., Ramstein, G. (2005) High-resolution simulations of the last glacial maximum climate over Europe: a solution to discrepancies with continental palaeoclimatic reconstructions? Climate Dynamics 24: 577-590.

Karátson, D., Telbisz, T, Harangi, Sz, Magyari, E., Dunkl, I., Kiss, B., Jánosi, Cs., Veres, D., Braun, M., Fodor, E., Biró, T., Kósik, Sz., von Eynatten, H., Lin, D. (2013) Morphometrical and geochronological constraints on the youngest eruptive activity in East-Central Europe at the Ciomadul (Csomád) lava dome complex, East Carpathians. Journal Of Volcanology and Geothermal Research 255(1): 43-56.

van der Knaap, W.O. (2009) Estimating pollen diversity from pollen accumulation rates: a method to assess taxonomic richness in the landscape. The Holocene 19: 159–164.

Kuneš, P., Pelánková, B., Chytrý, M., Jankovská, V., Pokorný, P. & Petr, L. (2008) Interpretation of the last-glacial vegetation of eastern-central Europe using modern analogues from southern Siberia. Journal of Biogeography 35: 2223–2236.

Kylander, M., Ampel, L., Wohlfarth, B., Veres, D. (2011) High-resolution X-ray fluorescence core scanning analysis of Les Echets (France) sedimentary sequence: new insights from chemical proxies. Journal of Quaternary Science 26: 109-117.

Legendre, P.L., Birks, H.J.B. (2012). From classical to canonical ordination. In: Birks, H. J. B., Lotter, A.F., Juggins, S. & Smol, J.P. (eds)Tracking Environmental Change Using Lake Sediments. Volume 5: Data Handling and Numerical Techniques. Springer, Dordrecht, pp. 201-248.

Liu, X., Colman, S.M., Brown, E.T., Minor, E.C., Li, H. (2013) Estimation of carbonate, total organic carbon, and biogenic silica content by FTIR and XRF techniques in lacustrine sediments. Journal of Paleolimnology 50: 387–398.

Magri, D., Vendramin, G.G., Comps, B., Dupanloup, I., Geburek, T., Gomory, D., Latalowa, M., Litt, T., Paule, L., Roure, J.M., Tantau, I., Van Der Knaap, W.O., Petit, R.J., De Beaulieu, J.L. (2006) A new scenario for the Quaternary history of European beech populations: palaeobotanical evidence and genetic consequences. New Phytologist 171: 199–221.Magyari, E., Jakab, G., Rudner, E. & Sümegi, P. (1999) Palynological and plant macrofossil data on Late Pleistocene short-term climatic oscillations in NE-Hungary. Acta Palaeobotanica. Supplement 2: 491-502.

Magyari, E. K., Buczkó, K., Jakab, G., Braun, M., Szántó, Zs., Molnár, M., Pál, Z., Karátson, D. (2006) Holocene palaeohydrology and environmental history in the South Harghita Mountains, Romania. Földtani Közlöny 136: 249-284.

Magyari, E. K., Buczkó, K., Jakab, G., Braun, M., Pál, Z., Karátson, D. (2009) Palaeolimnology of the last crater lake in the Eastern Carpathian Mountains - a multiproxy study of Holocene hydrological changes. Hydrobiologia, 631: 29-63.

Magyari, E.K., Jakab, G., Bálint, M., Kern, Z., Buczkó, K., Braun M. (2012) Rapid vegetation response to lateglacial and early Holocene climatic fluctuation in the South Carpathian Mountains (Romania). Quaternary Science Reviews 35(5):116–130.

Magyari, E.K., Kuneš, P., Jakab, G., Sümegi, P., Pelánková, B., Schäbitz, F., Braun, M., Chytrý, M. (2014) Late Pleniglacial vegetation in eastern-central Europe: are there modern analogues in Siberia? Quaternary Science Reviews 95: 60-79.

Major, C., Goldstein, S.L., Ryan,W., Lericolais, G., Piotrowski, A.M., Hajdas, I. (2006). The coevolution of Black Sea level and composition through the last deglaciation and its paleoclimatic significance. Quaternary Science Reviews 25: 2031–2047.

Manning, P.G., Murphy, T.P., Prepas, E.E. (1991) Intensive formation of vivianite in the bottom sediments of mesotrophic narrow lake, Alberta. Canadian Mineralogist 29: 77-85.

Markova, A.K., Simakova, A.N., Puzachenko, A.Y. (2009) Ecosystems of Eastern Europe at the time ofmaximumcooling of the Valdai glaciation (24–18 kyr BP) inferred from data on plant communities and mammal assemblages. Quaternary International 201: 53–59.

Marković, S.B., Bokhorst, M.P., Vandenberghe, J., McCoy, W.D., Oches, E.A., Hambach, U., Gaudenyi, T., Jovanović, M., Zöller, L., Stevens, T., Machalett, B. (2008) Late Pleistocene loessepalaeosol sequences in the Vojvodina region, north Serbia. Journal of Quaternary Science 23: 73-84.

Mîndrescu, M., Evans, I.S., Cox, N.J. (2010) Climatic implications of cirque distribution in the Romanian Carpathians: Palaeowind directions during glacial periods. Journal of Quaternary Science 25(6): 875–888.

Moore, P.D., Webb, J.A., Collinson, M.E. (1992) Pollen analysis. Second edition. Blackwell Scientific Publications, Oxford.

Moreno, A., Cacho, I., Canals, M., Grimalt, J.O., Sanchez-Vidal, A. (2011) Millennial-scale variability in the productivity signal from the Alboran Sea record, Western Mediterranean Sea. Palaeogeography, Palaeoclimatology, Palaeoecology 211 (3): 205-219.

Moreno, A., González-Sampériz, P., Morellón, M., Valero-Garcés, B. L., Fletcher, W.J. (2012) Northern Iberian abrupt climate change dynamics during the last glacial cycle: A view from lacustrine sediments. Quaternary Science Reviews 36: 139-153.

Müller, U.C., Pross, J., Tzedakis, P.C., Gamble, C., Kotthoff, U., Schmiedl, G., Wulf, S., and Christanis, K. (2011) The role of climate in the spread of modern humans into Europe. Quaternary Science Reviews 30: 273-279.

Naum Tr., Butnaru, E. (1989), Munții Căliman. Monografii Montane, Editura Sport-Turism, 232 p.

Novothny, Á., Frechen, M., Horváth, E., Wacha, L., Rolf, C. (2011) Investigating the penultimate and last glacial cycles of the Sütto loess section (Hungary) using luminescence dating, high-resolution grain size, and magnetic susceptibility data. Quaternary International 234: 75-85.

Obidowicz, A. (1996) A Late Glacial–Holocene history of the formation of vegetation belts in the Tatra Mts. Acta Palaeobotanica 36: 159–206.

Palmé, A.E., Vendramin, G.G. (2002) Chloroplast DNA variation, postglacial recolonization and hybridization in hazel, *Corylus avellana*. Molecular Ecology 11(9) 1769–1779.

Pál, Z. (2000) A Szent Anna Tó: következtetések a tó mélységét és feltöltődését illetően (Lake Saint Ana: inferences regarding water-depth and lake infillment). Collegicum Geographicum 1: 65-74.

Pál, Z. (2001) A Szent Anna Tó batimetriája (Bathymetry of Lake Saint Ana). Collegicum Geographicum 2: 73-78.

Panagiotopoulos, K., Böhm, A., Schäbitz, F. & Wagner, B. (2013) Climate variability since MIS 5 in SW Balkans inferred from multiproxy analysis of Lake Prespa sediments. Climate of the Past Discussions www.clim-past-discuss.net/9/1321/2013/cpd-9-1321-2013.html

Pandi, G. (2008) Morphometry of Lake Sfanta Ana, Romania (Lake Saint Ann). Lakes, reservoirs and ponds 1-2: 72-79. Romanian Limnogeographical Association.

Popa, M., Radulian, M., Szakács, A., Seghedi, I., Zaharia, B. (2011) New seismic and tomography data in the Southern part of the Harghita Mountains (Romania, Southeastern Carpathians): connection with recent volcanic activity. Pure and Applied Geophysics. http://dx.doi.org/10.1007/s00024-011-0428-6 (published online).

Provan, J., Bennett, K.D. (2008) Phylogeographic insights into cryptic refugia. Trends in Ecology and Evolution 23: 564–571.

Rasmussen, S.O., Andersen, K.K., Svensson, A.M., Steffensen, J.P., Vinther, B.M., Clausen, H.B., Siggaard-Andersen, M.-L., Johnsen, S.J., Larsen, L.B., Dahl-Jensen, D., Bigler, M., Röthlisberger, R., Fischer, H., Goto-Azuma, K., Hansson, M.E., Ruth, U. (2006) A new Greenland ice core chronology for the last glacial termination. Journal of Geophysical Research 111, D6.

Rasmussen, S. O., M. Bigler, S. Blockley and. T. Blunier, S. L. Buchardt, H. B. Clausen, I. Cvijanovic, D. Dahl-Jensen, S. J. Johnsen, H. Fischer, V. Gkinis, M. Guillevic, W. Hoek, J. J. Lowe, J. Pedro, T. Popp, I. E. Seierstad, J. P. Steffensen, A. M. Svensson, P. Vallelonga, B. M. Vinther, M. J. Walker, J. Wheatley, M. Winstrup (2014) A stratigraphic framework for robust naming and correlation of past abrupt climatic changes during the last glacial period based on three synchronized Greenland ice core records. Quaternary Science Reviews. in press

Reille, M. (1992) Pollen et spore D'Europe et D'Afrique du Nord. Laboratorie de Botanique Historique et Palynologie Marseille, France.

Reille, M. (1995) Pollen et spore D'Europe et D'Afrique du Nord. Supplement 1. Laboratorie de Botanique Historique et Palynologie Marseille, France.

Reille, M. (1998) Pollen et spore D'Europe et D'Afrique du Nord. Supplement 2. Laboratorie de Botanique Historique et Palynologie Marseille, France.

Reimer, P. J., Bard, E., Bayliss, A., Beck, J. W., Blackwell, P. G., Bronk Ramsey, C., Grootes, P. M., Guilderson, T. P., Haflidason, H., Hajdas, I., Hatté, C., Heaton, T. J., Hoffmann, D. L., Hogg, A. G., Hughen, K. A., Kaiser, K. F., Kromer, B., Manning, S. W., Niu, M., Reimer, R. W., Richards, D. A., Scott, E. M., Southon, J. R., Staff, R. A., Turney, C. S. M., & van der Plicht, J. (2013). IntCal13 and Marine13 Radiocarbon Age Calibration Curves 0-50,000 Years cal yr BP. Radiocarbon 55(4): 1869-1887.

Renssen, H., Isarin, R.F.B. (2001) The two major warming phases of the last deglaciation at ~ 14.7 and ~ 11.5 ka cal. BP in Europe: climate reconstruction and AGCM experiments. Global and Planetary Change 30: 117-153.

Renssen, H., and Osborn, T.J. (2003) Investigating Holocene climate variability: data-model comparisons. PAGES Newsletter 11 (2-3), 32-33.

Rethemeyer, J., Fülöp, R. H., Höfle, S., Wacker, L., Heinze, Hajdas, S. I., Patt, U., König, S., Stapper, B., Dewald, A. (2013) Status report on sample preparation facilities for ^{14}C analysis at the new CologneAMS center. Nuclear Instruments and Methods in Physics Research Section B: Beam Interactions with Materials and Atoms 294: 168-172.

Ronikier, M., Cieślak, E., Korbecka, G. (2008a) High genetic differentiation in the alpine plant *Campanula alpina* Jacq. (Campanulaceae): Evidence for glacial survival in several Carpathian regions and long-term isolation between the Carpathians and the Alps. Molecular Ecology 17: 1763–1775.

Ronikier, M., Costa, A., Fuertes Aguilar, J., Nieto Feliner, G., Küpfer, P. & Mirek, Z. (2008b) Phylogeography of *Pulsatilla vernalis* (L.) Mill. (Ranunculaceae): Chloroplast DNA reveals two evolutionary lineages across central Europe and Scandinavia. Journal of Biogeography 35: 1650–1664.

Rostek, F, Bard, E. (2013) Hydrological changes in eastern Europe during the last 40,000 years inferred from biomarkers in Black Sea sediments. Quaternary Research 80: 502-509.

Schmitt, T., Varga, Z. (2012) Extra-Mediterranean refugia: The rule and not the exception? Frontiers in Zoology 9:22.

Seppä, H., Hicks, S. (2006) Using modern and past pollen accumulation rate (PAR) records to reconstruct and map past tree-line patterns: a method for more precise vegetation reconstructions. Quaternary Science Reviews 25: 1501-1516.

Shumilovskikh, L., Tarasov, P., Arz, H.W., Fleitmann, D., Marret, F., Nowaczyk, N., Plessen, B., Schlütz, F., Behling, H. (2012) Vegetation and environmental dynamics in the southern Black Sea region since 18 kyr BP derived from the marine core 22-GC3. Palaeogeography, Palaeoclimatology, Palaeoecology 337-338: 177-193.

Soulet, G., Ménot, G., Bayon, G., Rostek, F., Ponzevera, E., Toucanne, S., Lericolais, G., Bard, E. (2013) Abrupt drainage cycles of the Fennoscandian Ice Sheet. Proceedings of the National Academy of Science 110 (17): 6682–6687.

Stevens, T., Markovićc, S.B., Zech, M., Hambach, U., Sümegi, P., 2011. Dust deposition and climate in the Carpathian Basin over an independently dated last glaciale interglacial cycle. Quaternary Science Reviews 30: 662-681.

Stewart, J.R., Lister, A.M. (2001) Cryptic northen refugia and the origins of modern biota. Trends in Ecology and Evolution 16: 608-613.

Strandberg, G., Brandefelt, J., Kjellström, E., Smith, B. (2011) High-resolution regional simulation of last glacial maximum climate in Europe. Tellus A, North America, 63, Available at: <http://www.tellusa.net/index.php/tellusa/article/view/15773>. Date accessed: 18 June 2014.

Sugita, S. (2007) Theory of quantitative reconstruction of vegetation. I. Pollen from large sites REVEALS regional vegetation composition . The Holocene 17: 229 - 241.

Sümegi, P., Magyari, E., Dániel, P., Molnár, M., Törőcsik, T. (2013) Responses of terrestrial ecosystems to Dansgaard-Oeshger cycles and Heinrich-events: a 28,000-year record of environmental changes from SE Hungary. Quaternary International 293: 34–50.

Svenning, J.-C., Normand, S., Kageyama, M. (2008) Glacial refugia of temperate trees in Europe: insights from species distribution modelling. Journal of Ecology 96: 1117–1127.

Szakács, A., Seghedi, I., Pécskay, Z. (2002) The most recent volcanism in the Carpathian–Pannonian region. Is there Any Volcanic Hazard? Geologica Carpathica Special Issue, Proceedings of the XVIIth Congress of Carpatho-Balkan Geological Association 53: 193–194.

Tămaş , T., Onac, B.P. & Bojar, A.V. (2005) Lateglacial–Middle Holocene stable isotope records in two coeval stalagmites from the Bihor Mountains, NW Romania. Geological Quarterly 49: 185–194.

Tanţău I., Reille M., de Beaulieu J.L., Farcas S., Goslar T., Paterne M. (2003) Vegetation history in the eastern Romanian Carpathians: pollen analysis of two sequences from the Mohoş crater. Vegetation History and Archaeobotany 12: 113–125.

Tanţău, I., Reille, M., de Beaulieu, J.L. & Fărcaş, S. (2006) Late Glacial and Holocene vegetation history in the southern part of Transylvania (Romania): pollen analysis of two sequences from Avrig. Journal of Quaternary Science 21: 49–61.

Tanţău, I., Feurdean, A., Beaulieu, J.L. de, Reille, M., Fărcaş, S. (2011) Holocene vegetation history in the upper forest belt of the Eastern Romanian Carpathians. Palaeogeography, Palaeoclimatology, Palaeoecology 309: 281-290.

Tanţău, I., Feurdean, A., de Beaulieu, J.L., Reille, M., Farcas, S. (2014) Vegetation sensitivity to climate changes and human impact in the Harghita Mountains (Eastern Romanian Carpathians) over the past 15 000 years. Journal of Quaternary Science 29: 141-152.

Tasenkevich, L. (1998) Flora of the Carpathians. Checklist of the native vascular plant species. State Museum of Natural History, Nacional Na Akademija Nank Ukrainy, L'viv, 609 p.

Tinner, W., Hubschmid, P., Wehrli, M., Ammann, B., Conedera, M., 1999. Long-term forest fire ecology and dynamics in southern Switzerland. Journal of Ecology 87: 273–289.

Tzedakis, P.C. (1999) The last climatic cycle at Kopais, central Greece. Journal of the Geological Society, London 155: 425-434.

Tzedakis, P.C., Lawson, I.T., Frogley, M.R., Hewitt, G.M., Preece, R.C. (2002) Buffered tree population changes in a quaternary refugium: evolutionary implications. Science 297: 2044-2047.

Tzedakis, P. C., Roucoux, K. H., de Abreu, L. & Shackleton, N. J. (2004) The duration of forest stages in southern Europe and interglacial climate variability. Science 306: 2231-2235.

Tzedakis, P.C., Emerson, B.E. & Hewitt, G.M. (2013) Cryptic or mystic? Glacial tree refugia in northern Europe. Trends in Ecology and Evolution 28: 696-704. 0.1016/j.tree.2013.09.001.

Újvári, G., Kovács, J., Varga, G., Raucsik, B., Marković, S.B. (2010) Dust flux estimates for the Last Glacial Period in East Central Europe based on terrestrial records of loess deposits: a review. Quaternary Science Reviews 29: 3157-3166.

Ujvárosi, L., Nógrádi, S., Uherkovich, Á. (1995) Studies on the Trichoptera fauna of the Ciuc Basin and Harghita Mountains, Romania. Folia Historico Naturalia Musei Matraensis 20: 99-113.

Urdea, P. (2004) The Pleistocene glaciation of the Romanian Carpathians. In: Ehlers, J., Gibbard, P.L. (eds), Quaternary Glaciations-Extent and Chronology, Part I. Elsevier, Amsterdam, pp. 301-308.

Urdea, P., Onaca, A., Ardelean, F., Ardelean, M. (2011) New Evidence on the Quaternary Glaciation in the Romanian Carpathians. Developments in Quaternary Science 15: 305-322.

Vandenberghe, J., Renssen, H., Roche, D.M.V.A.P., Goosse, H.J.M., Velichko, A.A., Gorbunov, A. & Levavasseur, G. (2012) Eurasian permafrost instability constrained by reduced sea-ice cover. Quaternary Science Reviews 34: 16-23.

Varsányi, I., Palcsu, L., Kovács, L.Ó. (2011) Groundwater flow system as an archive of palaeotemperature: noble gas, radiocarbon, stable isotope and geochemical study in the Pannonian Basin, Hungary. Applied Geochemistry 26: 91-104.

Veres, D., Lallier-Verges, E.,Wohlfarth, B., Lacourse, T., Keravis, D., Bjorck, S., Preusser, F., Andrieu-Ponel, V., Ampel, L. (2009) Climate-driven changes in lake conditions during late MIS 3 and MIS 2: a high-resolution geochemical record from Les Echets, France. Boreas 38, 230–243.

Vescovi, E., Ravazzi, C., Arpenti, E., Finsinger, W., Pini, R., Valsecchi, V., Wick, L., Ammann, B., Tinner, W., 2007. Interactions between climate and vegetation during the Lateglacial period as recorded by lake and mire sediment archives in Northern Italy and Southern Switzerland. Quaternary Science Reviews 26: 1650-1669.

Willis, K.J., Rudner E., Sümegi, P. (2000) The Full-Glacial Forests of Central and Southeastern Europe. Quaternary Research 53: 203-213.

Willis, K.J. , van Andel, T.H. (2004) Trees or no trees? The environments of central and eastern Europe during the Last Glaciation. Quaternary Science Reviews 23: 2369–2387.

Zech, R., Zech, M., Marković, S., Hambach, U., Huang, Y. (2013) Humid glacials, arid interglacials? Critical thoughts on pedogenesis and paleoclimate based on multi-proxy analyses of the loess–paleosol sequence Crvenka, Northern Serbia. Palaeogeography, Palaeoclimatology, Palaeoecology 387: 165-175.

Figure legend

Figure 1 Topographic map showing the location of Lake St Anne within East-Central Europe (a) and within the Ciomadul Mountains (b). Elevation gradients within the Ciomadul Mountains are shown along three transects.

Figure 2 Age-depth model for core SZA-2010 (1700-950 cm depth), Lake St Anne, Romanian Carpathians. Two age depth models are shown: the Bayesian model (a) takes into account all radiocarbon dates; while the linear model (b) excludes one radiocarbon date from 1092 cm.

Figure 3 Lithology, lithozones (LZ), magnetic susceptibility (MS), titanium (Ti), iron (Fe), calcium (Ca) and sulphur (K) intensities (10^3 counts), organic content (LOI%), major vegetation types (% pollen data), depth and age (cal yr BP) of core SZA-2010 from Lake St Anne (1682-970 cm depth). Dashed lines in the figure mark major changes in the MS and XRF element data. In the summary percentage pollen diagram each pollen type was assigned to a major vegetation type following a simple biome scheme (Feurdean et al., 2014).

Figure 4 Relative frequencies of selected terrestrial pollen types from core SZA-2010, Lake St Anne, Romanian Carpathians (ca. 6200-26,400 cal yr BP). Results of the rarefraction analysis $E(T_{350})$ reflecting palynological richness, microcharcoal accumulation rates and terrestrial pollen accumulation rates are alos shown on the right. LPAZ: local pollen assemblage zones.

Figure 5 Relative frequencies of selected wetland and aquatic pollen types and non-pollen palynomorphs (algae and Sordaidaceae fungal spores) from core SZA-2010, Lake St Anne, Romanian Carpathians (ca. 6200-26,400 cal yr BP). LPAZ: local pollen assemblage zones.

Figure 6 Pollen accumulation rates (pollen cm-2 yr-1) of major terrestrial pollen types from Lake St Anne, core SZA-2010. Local pollen assemblage zone (LPAZ) descriptions are given in Table 1.

Figure 7 Results of the principal component analysis (PCA) for which we used the 30 most abundant terrestrial pollen types from core SZA-2010, Lake St Anne (samples between 971 and 1676 cm). SZA-1 to SZA-6 are pollen assemblage zones according to Figure 4 and Table 2.

Figure 8 High-resolution paleovegetation and magnetic susceptibility records of core SZA-2010, lake St Anne, Romanian Carpathians compared to (a) the $\delta^{18}O$ record of NGRIP ice core (Andersen et al., 2004), to (b) the composite atmospheric CH_4 record from Greenland (Blunier et al., 2007) and to (c) the Sofular cave stalagmite $\delta^{13}C$ record (Gögtürk et al., 2011). (d) Magnetic susceptibility as indicator of aeolian dust accumulation during the LGM (not reversed scale); (e) Pinus pollen percentages; (f) Xerophytic steppe representation; (g) DCCA axis one scores as a measure of pollen compositional change and thereby the magnitude of vegetation change. HE: Heinrich-event; DO: Dansgaard-Oeschger event; GI: Greenland interstadial; GS: Greenland stadial.

Supplementary material

Supplementary Table 1 List of pollen types included in the calculation of major vegetation types (biomes) around Lake St Anne. Each pollen type was assigned to one of these biomes.

Supplementary Table 2 Sediment stratigraphy of core SZA-2010, Lake St Anne (Lake Sfanta Ana), Harghita Mts, Romania. Note that sediment depths shown in this table include 600 cm water depth; sediment stratigraphy of the 600-950 cm sediment section representing the middle and late Holocene was described elsewhere (Magyari et al., 2006, 2009).

Supplementary Figure 1 Photo of the 1000-1095 cm sediment section from Lake St Anne with Fe intensities (10^3 count), core SZA-2010.

Supplementary Figure 2 Grain size distribution in core SZA-2010 as measured by laser particle analyser.

Supplementary Figure 3 Relative frequencies of all terrestrial pollen types from Lake St Anne, core SZA-2010 plotted against depth (cm). LPAZ: local pollen assemblage zones.

Table 1 AMS radiocarbon dates and from Lake St Anne, core SZA-2010. Depths, materials chosen as well as radiocarbon ages and calendar ages are given. The radiocarbon ages of all samples were calibrated into calendar years before present (cal yr BP) using the INTCAL13 calibration curve (Reimer et al., 2013).

Depth (cm)	Lab code	Material dated	conv. age (yr BP)	±	Calibrated range BP (2σ)	Age (cal BP) age used for linear modelling	±	Carbon weight (mg)	Remarks
980-982	COL1116.1+2.1	*Sphagnum* leaves and stems, *Picea* abies needles, bract *scales*	6246	26	7155–7258	7206.5	51.5	1	
1000-1002	COL1117.1+2.1	moss leaves and stems, bract scales, periderm	8216	28	9082–9286	9184	102	1	
1036-1038	COL1118.1+2.1	Charcoal, moss stems, periderm, bract scale	10739	42	12,562–12,742	12652	90	0.58	
1072-1073	COL1119.1.1	micro & macrocharcoal	14038	38	16,830–17,263	17046.5	216.5	1	
1091-1092	COL1121.2.1	herb stems, likely Cyperaceae stem	15400	44	18,556–18,784	18670	114	1	rejected in linear model
1126-1127	COL1122.2.1	Cyperaceae stem/leaf fragments	14541	67	17,371–17,976	17673.5	302.5	0.26	
1340-1342	COL1123.1.+2.1	Charcoal Cyperaceae stem fragments, chironomid head capsules, Cladocera egg	17338	84	20,290–21,138	20714	424	0.28	
1365-1366	COL1124.1+2.1	Cyperaceae stem fragments, chironomid head capsules, Cladocera egg	17626	96	20,523–21,387	20955	432	0.18	
1538-1540	COL1127.1.+2.1	Moss leaves, stems, chironomid head capsules, Cladocera egg	19717	122	23,133–23,953	23543	410	0.13	
1661-1662	COL1128.1.1	Cladocera egg	21685	163	25400–26713	26056.5	656	0.09	

Zone	Depth/Age cm/cal yr BP	Zone characteristics (Figs 4 & 5, ages are according to the linear model) Terrestrial	 Aquatic & NPP		AP %	CHAR	PAR	PAL RICH
SZA-1	1676-1493.5 linear model: 26,350-22,870 Bayesian model: 25,965-23,025	*Pinus* (12-45%) and *Juniperus* (8-15%) dominate woody taxa; haplo- and diploxylon pines are present; other characteristic trees are *Betula*, *Picea abies*, *Larix*, *Quercus* and *Corylus*, *Hippophaë rhamn*.; herbs are dominated by Poaceae (22-35%), Artemisia (5-17%), Chenopodiaceae, Caryophyllaceae and Asteraceae; charcateristic herbs are *Plantago* m/m., *Rumex*, *Helianthemum*, *Polygonum viviparum*, *Soldanella*, *Jasione*, *Galium*; *Thalictrum* shows a peak at 1526 cm (23,350 cal yr BP); one degraded conifer stomata was found at 1628 cm (25,370 cal yr BP); inferred vegetation: the crater slopes were likely not wooded, regional presence of hemiboreal and taiga forests/forest steppes are inferred; *Juniperus* was likely present in the mountains, crater slope was likely covered with alpine/tundra and ruderal herbs; overall vegetation cover was low	Very few aquatic taxa, occasional occurrence of *Typha ang*., *Rincospora*, *Equisetum*, *Sphagnum*; green alge are represented by few *Botryococcus*, *Spyrogyra* and *Pediastrum* remains; some Cypearaceae likely of wetland origin; species poor shallow, likely seasonal or year-round ice-covered lake is inferred with Cypearaceae on the shore	max. min. av.	57 24 42	721 61 265	2705 432 1270	26 15 21
SZA-2	1493.5-1230 linear model: 22,870-19,150 Bayesian model: 23,025-19,140	*Pinus* percentages are high (40-50%) between 22,000-23,000 cal yr BP, then decrease to 10-20%; *Corylus*, *Ulmus*, *Fraxinus exc*., *Fagus sylv*., *Carpinus betulus*, *Salix* increase or more often recorded; note their peak values at 1493 cm (22,860 cal yr BP); *Juniperus* high (10-20%); *Ephedra* more often recorded; *Artemisia* decreases (10→ 3%); Poaceae increases above 1355 cm (20,860 cal yr BP); characteristic herbs are *Thalictrum*, *Armeria*, *Ranunculus*, *Aconitum*, *Saxifraga*, *Cardamine*, *Scrophularia*-type, *Valeriana* off., Apiaceae, *Hypericum*, *Helleborus*; regionally increasing woody cover is inferred and increased regional forest fires; temperate deciduous trees/shrubs were likely present at lower altitude; locally increased vegetation cover in the crater, tall forbs and cushion-forming herbs spread likely on wet and stony surfaces, xerophytic steppe cover decreased, grass steppes dominated	Sudden increase in *Botryococcus*; Polypodiaceae, *Pediastrum*, *Spyrogyra* and Zygnemataceae also increase; Cyperaceae decrease; shallow, dystrophic lake is inferred with slight increase in nutrient availability; ferns likely originate from regional pollen rain	max. min. av.	75 30 52	5814 269 1698	7549 1025 3103	33 18 25
SZA-3	1230-1073 linear model: 19,150-14,600 Bayesian model: 19,140-16,010	*Pinus* fluctuates between 20-50%; deciduous temperate taxa are present, but less abundant; *Betula* and *Pinus* increase in SZA-3b (1103 cm, 16,310 cal yr BP); *Artemisia* and Chenopodiaceae increase significantly, while Poaceae and *Juniperus* decrease; note that *Juniperus* re-increases between 1139-1107 cm (17,830-17,070 cal yr BP); typical herb pollen types are *Polygonum viviparum*, *Soldanella*, *Trientalis*, *Sangusiorba officinalis*, *Dryas octopetala;* inferred vegetation change: expansion of xerophytic/*Artemisia* steppes against grass steppes and juniper scrubland at ~19,150 cal yr BP; pine-birch forests spread regionally from 1107 cm (16,500 cal yr BP); overall veg. cover increased; locally alpine/tundra and wet meadow herbs spread in the crater; regional fire activity decreased; re-expansion of *Juniperus* may indicate cooling during Heinrich-event 1	rapid increase in *Pediastrum*; *Rincospora*, *Equisetum*, *Potamogeton*, *Miryophyllum vert*., Pinguicalula are present; *Botryococcus*, *Pediastrum*, *Secenedesmus* further increase in SZA-3b; inferred vegetation in the lake becomes richer in green algae and suggests increasing lake levels and/or nutrient levels, with further lake level rise in SZA-3b	max. min. av.	67 38 51	998 90 467	6379 1525 3314	28 13 21
SZA-4	1073-1033 linear model: 14,600-12,300 Bayesian model: 16,010-12,290	*Pinus* increases rapidly (50→70%); *Larix*, *Picea* and *Betula* are important tree taxa; *Juniperus* (10→2%), *Artemisia* (), Chenopodiaceae decrease rapidly at 1071 cm (14,540 cal yr BP); *Polygonum viviparum*, Caryophyllaceae, *Potentilla*, *Dryas*, *Helianthemum* disappear/decrease; *Epilobium* appears; in SZA-4b (1047-1033 cm, 13,300-12,300) *Artemisia* and Poaceae increase, while *Pinus*, *Betula* and *Picea* decrease; inferred vegetation change involves the regional expansion of hemiboreal pine-birch and larch forests and spruce taiga at the expense of xerophytic steppes; re-expansion of steppes likely indicate decreasing available moisture and may correspond to the YD event; regional fire activity increased	Disappearance/decrease of green algae in SZA-4a followed by re-appearance of the same taxa in SZA-4b; *Scenedesmus* high in SZA-4b, Sordaidaceae spores appear first; lake-level likely decreased rapidly in SZA-4a; lake level likely increased in SZA-4b concurrently with the AP decline	max. min. av.	89 54 77	9553 1076 3188	37657 3214 9703	19 11 17
SZA-5	1033-1021 linear model: 12,300-11,100 Bayesian model: 12,290-11,160	*Ulmus* (1.6→10%) and *Betula* (5-32%) increase rapidly followed by increases in *Fraxinus exc*., *Corylus* and *Quercus*; *Pinus* decreases at 1031 cm (12,070 cal yr BP), while *Betula* decrease in the second part of the zone; following initial afforestation by early successional birch trees, forest expanded at elevations below 1000 m; the crater slopes also became forested (locally birch and spruce were likely important)	rapid increase in *Botryococcus*; *Pediastrum* disappears; *Scenedesmus* has similar values than in SZA-4b; telmatophytes disappear; the lake became warmer & shallower, pH decreased	max. min. av.	89 84 86	3862 1730 2606	13516 4110 8039	16 12 14
SZA-6	1021-971 linear model: 11,100-6200 Bayesian model: 11,160-6200	*Ulmus*, *Fraxinus*, *Quercus*, *Tilia*, *Picea*, *Corylus* dominate the pollen assemblages regionally we infer the maximum development of mixed deciduous forests; regionally *Picea abies* appeared on the lakeshore (Magyari et al. 2006, 2009)	Sordaidaceae spores dominate; *Botryococcus* and *Zygnemataceae* are abundant; testate amoebae are present; *Sphagnum* dominated shallow hollows and pools are inferred locally; Sordaidaceae likely grew on woods/shrubs falling down the lake	max. min. av.	96 88 94	18150 524 3322	21779 5 9928 41881	22 12 15

Table 2 Pollen assemblage zone characteristics of core SZA-2010, Lake St Anne, Romanian Carpathians.

Depth (cm)	Age cal yr BP (linear model)	Plant macrofossils
1050	13370	*Sphagnum* sec. Cuspidata leaf (1)
1051	13430	*Betula pubescens* seed (1), *Equisetum fluviatile* epidermis fragments (many, >100), *Warnstorfia fluitans* leaf (1), *Sphagnum* sec. Cuspidata leaves (2)
1074	14705	*Pinus sylvestris needle (1); Pinus sylvestris epidermis (1)*
1081	15095	cf. *Scheuchzeria* epidermis fragments
1082	15150	*Betula nana* seed (1), *Betula pubescens* seed (1), *Carex* sp. achene fragment (1), *Polytrichum* sp. leaf (1)
1091	15650	*Typha minima* seed (1), UI Cyperaceae stems (several)
1092	15705	UI Cyperaceae stems (several), macrocharcoal (several)
1111	16760	identifiable plant macrofossils were not found
1112	16815	identifiable plant macrofossils were not found
1352	20830	UI macrocharcoal
1375	21115	UI moss stems
1430	21930	UI macrocharcoal

Table 3 Plant macrofossils in selected sediment samples of Lake St Anne, core SZA-2010, Ciomadul Mts, Romania. Note that tree/shrub macrofossils were not detected below 1082 cm (15,150 cal yr BP). Numbers in brackets after the taxon name indicate number of fossil findings. UI: unidentifiable.

Figure 01

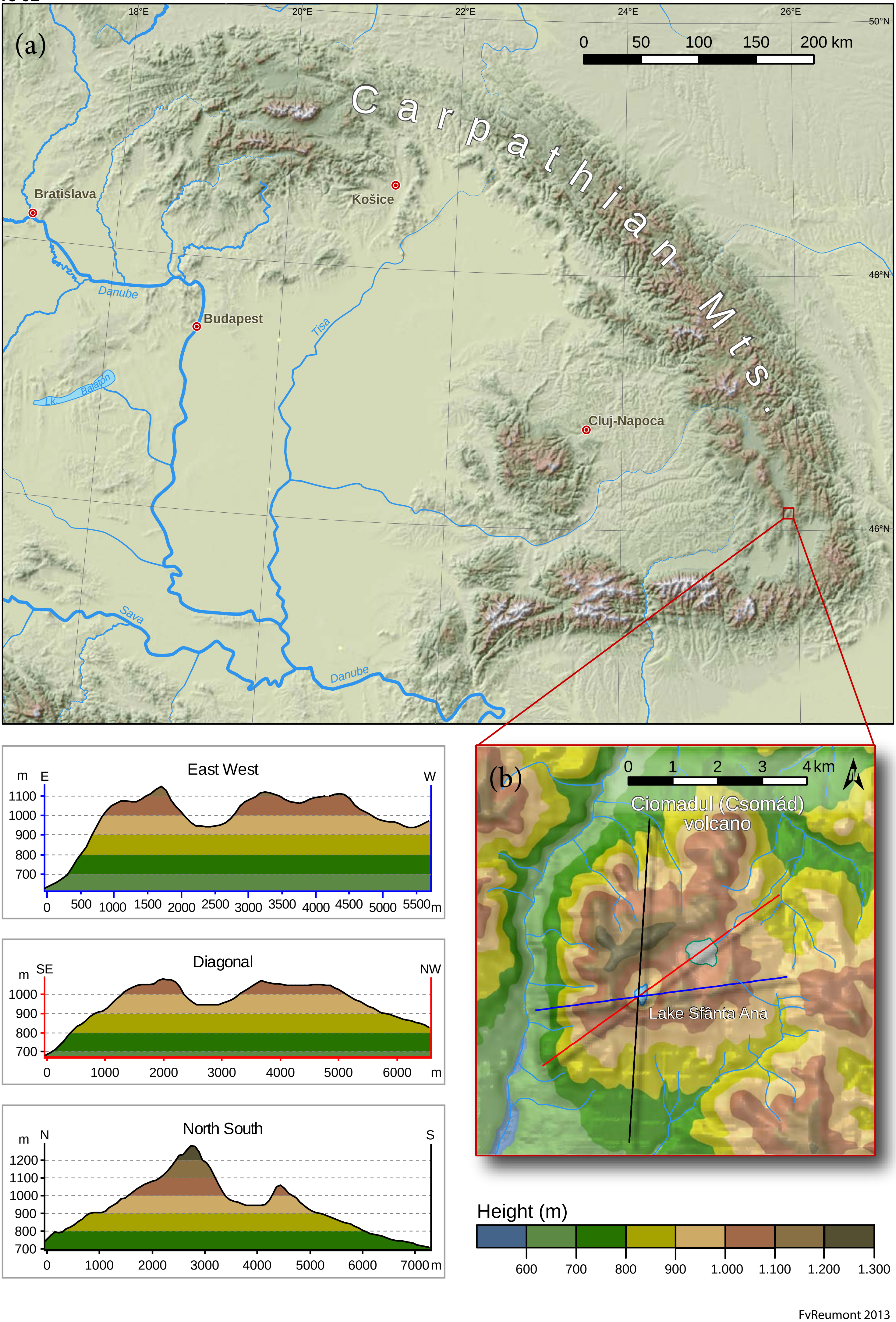
(a)
18°E
20°E
22°E
24°E
26°E
50°N
48°N
46°N
0 50 100 150 200 km
Carpathian Mts.
Bratislava
Košice
Budapest
Cluj-Napoca
Danube
Tisa
Lk. Balaton
Sava
Danube
East West
m E W
1100 1000 900 800 700
0 500 1000 1500 2000 2500 3000 3500 4000 4500 5000 5500 m
Diagonal
m SE NW
1000 900 800 700
0 1000 2000 3000 4000 5000 6000 m
North South
m N S
1200 1100 1000 900 800 700
0 1000 2000 3000 4000 5000 6000 7000 m
(b)
0 1 2 3 4 km
Ciomadul (Csomád) volcano
Lake Sfânta Ana
Height (m)
600 700 800 900 1.000 1.100 1.200 1.300
FvReumont 2013

Figure 02

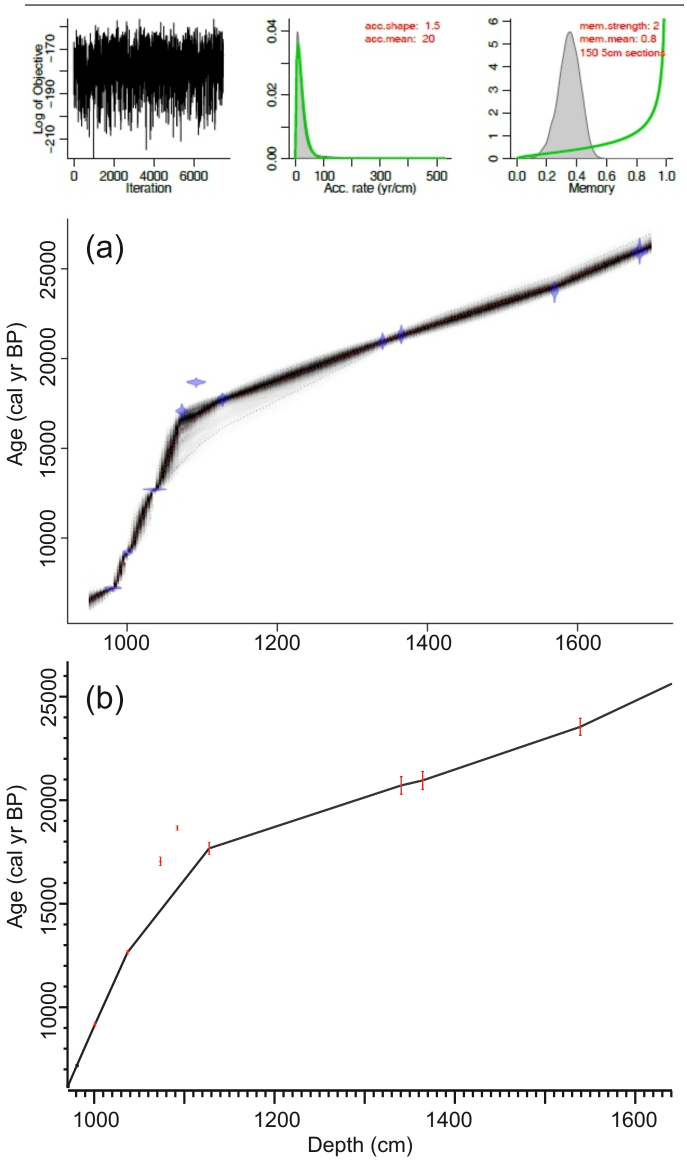

Log of Objective
-210
-190
-170
0
2000
4000
6000
Iteration
0.00
0.02
0.04
acc.shape: 1.5
acc.mean: 20
0
100
300
500
Acc. rate (yr/cm)
0
1
2
3
4
5
6
mem.strength: 2
mem.mean: 0.8
150 5cm sections
0.0
0.2
0.4
0.6
0.8
1.0
Memory
(a)
Age (cal yr BP)
10000
15000
20000
25000
1000
1200
1400
1600
(b)
Age (cal yr BP)
10000
15000
20000
25000
1000
1200
1400
1600
Depth (cm)

Figure 03
Click here to download high resolution image

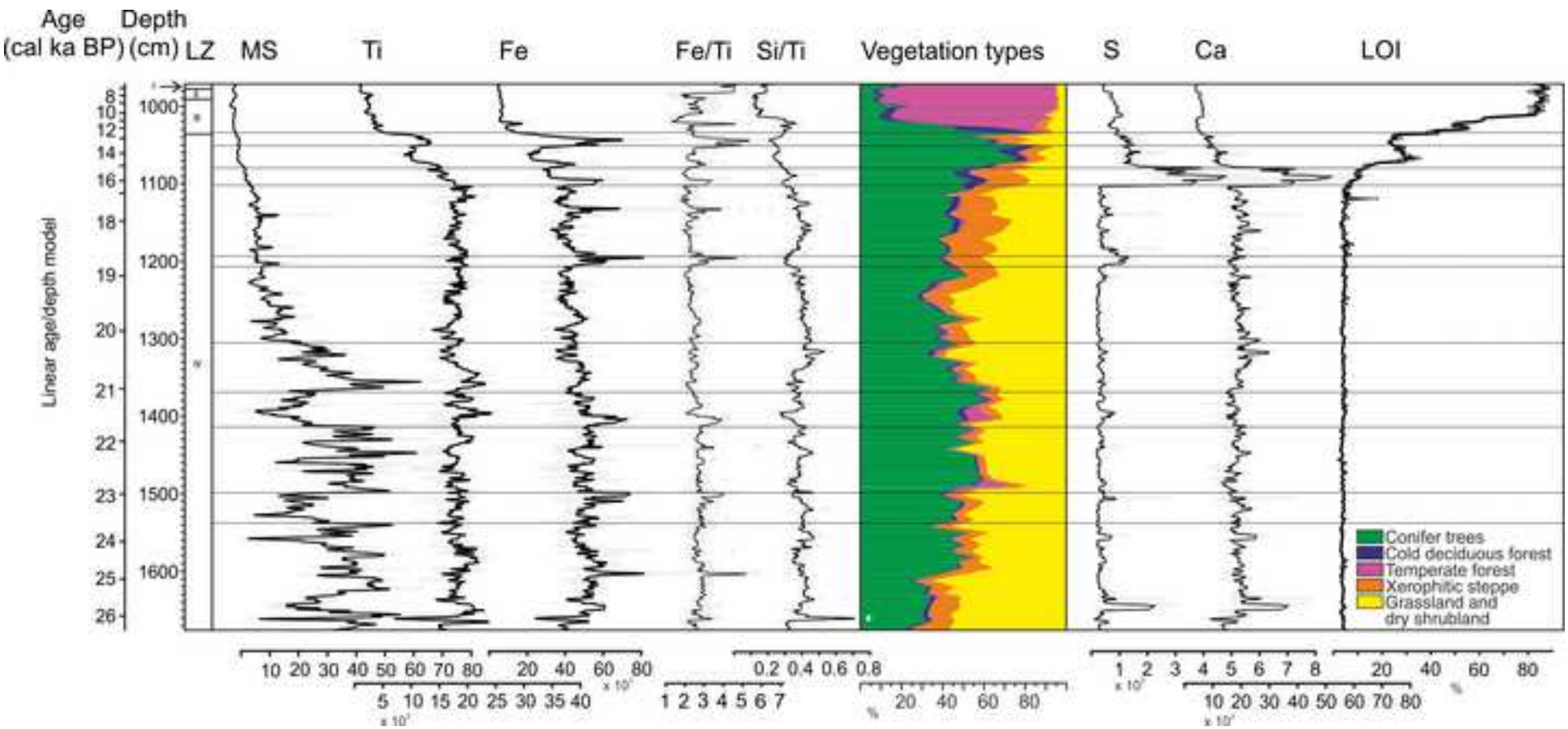

Figure 04

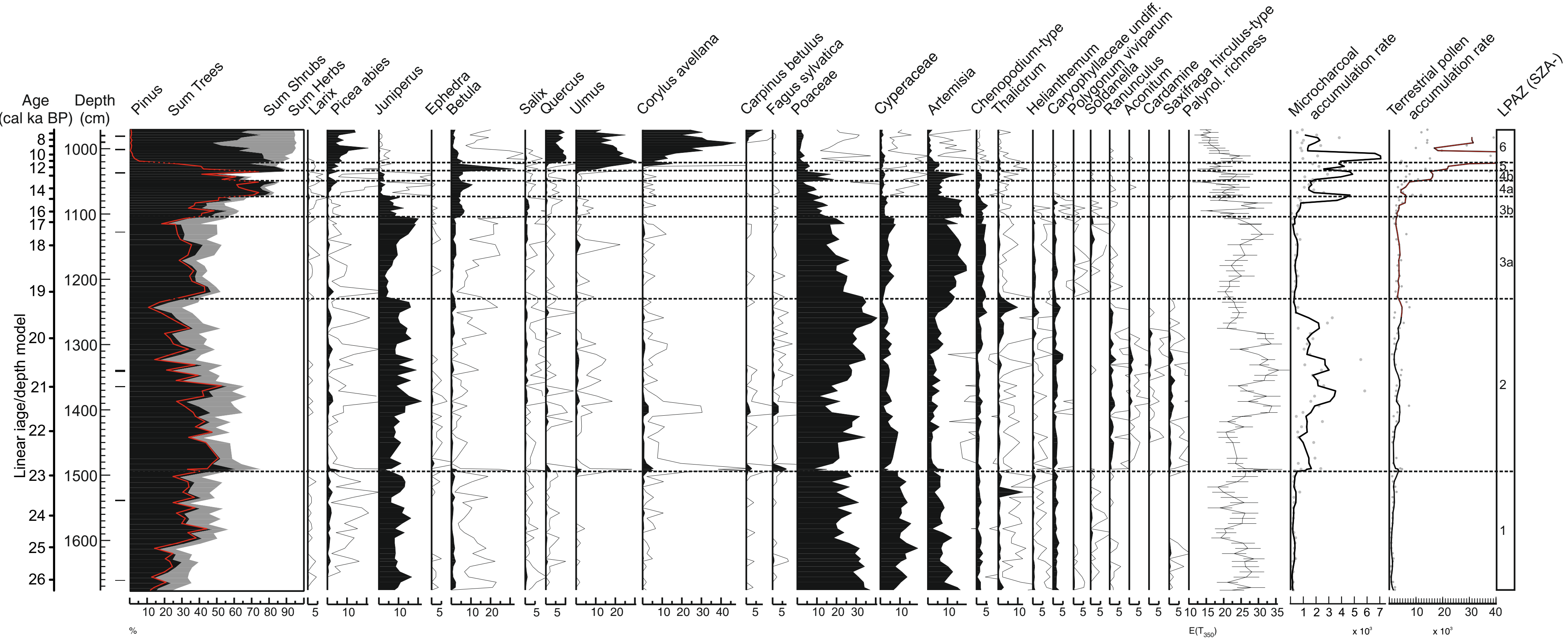

Age (cal ka BP)
Depth (cm)
Linear iage/depth model
Pinus
Sum Trees
Sum Shrubs
Sum Herbs
Larix
Picea abies
Juniperus
Ephedra
Betula
Salix
Quercus
Ulmus
Corylus avellana
Carpinus betulus
Fagus sylvatica
Poaceae
Cyperaceae
Artemisia
Chenopodium-type
Thalictrum
Helianthemum
Caryophyllaceae undiff.
Polygonum viviparum
Soldanella
Ranunculus
Aconitum
Cardamine
Saxifraga hirculus-type
Palynol. richness
Microcharcoal accumulation rate
Terrestrial pollen accumulation rate
LPAZ (SZA-)
%
E(T350)
x 10³
x 10³
6
5
4b
4a
3b
3a
2
1

Figure 05

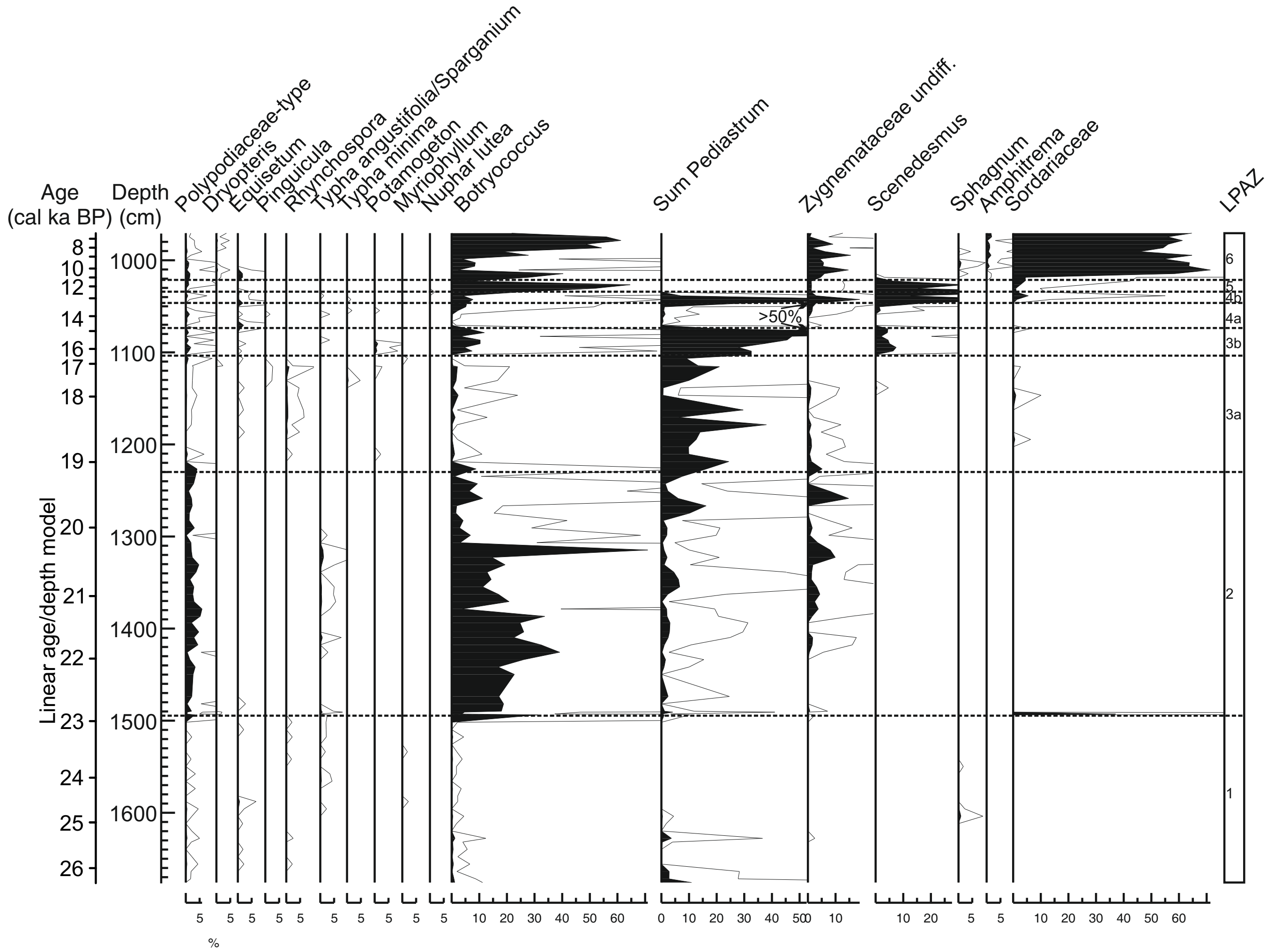

Age (cal ka BP)
Depth (cm)
Polypodiaceae-type
Dryopteris
Equisetum
Pinguicula
Rhynchospora
Typha angustifolia/Sparganium
Typha minima
Potamogeton
Myriophyllum
Nuphar lutea
Botryococcus
Sum Pediastrum
Zygnemataceae undiff.
Scenedesmus
Sphagnum
Amphitrema
Sordariaceae
LPAZ
Linear age/depth model
>50%
%

Figure 06

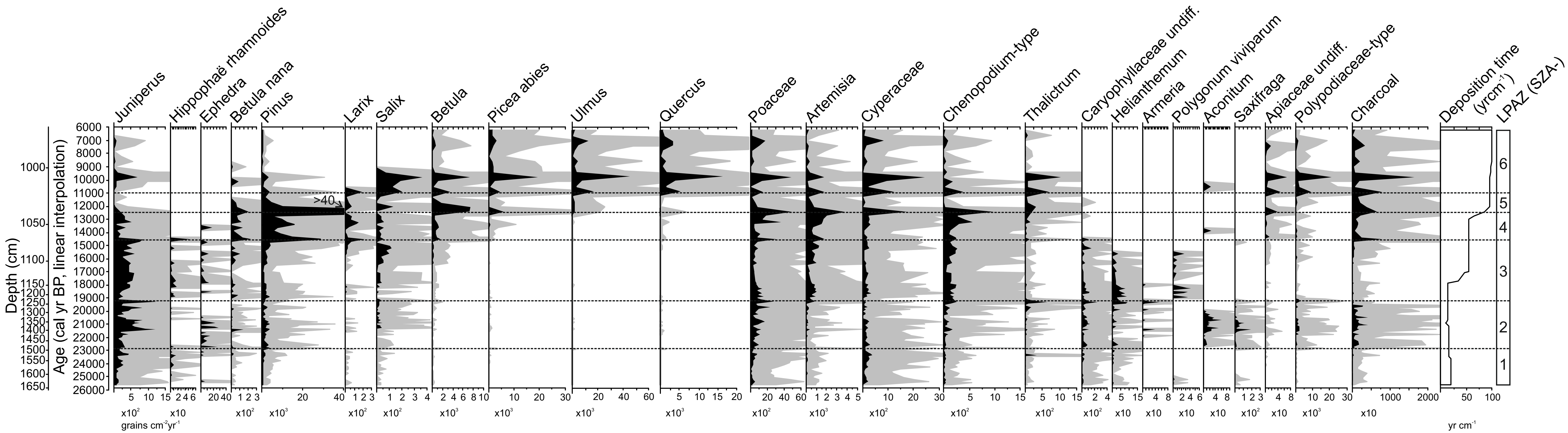

Juniperus
Hippophaë rhamnoides
Ephedra
Betula nana
Pinus
Larix
Salix
Betula
Picea abies
Ulmus
Quercus
Poaceae
Artemisia
Cyperaceae
Chenopodium-type
Thalictrum
Caryophyllaceae undiff.
Helianthemum
Armeria
Polygonum viviparum
Aconitum
Saxifraga
Apiaceae undiff.
Polypodiaceae-type
Charcoal
Deposition time (yrcm-1)
LPAZ (SZA-)
Depth (cm)
Age (cal yr BP, linear interpolation)
>40
grains cm-2yr-1
yr cm-1

Figure 07

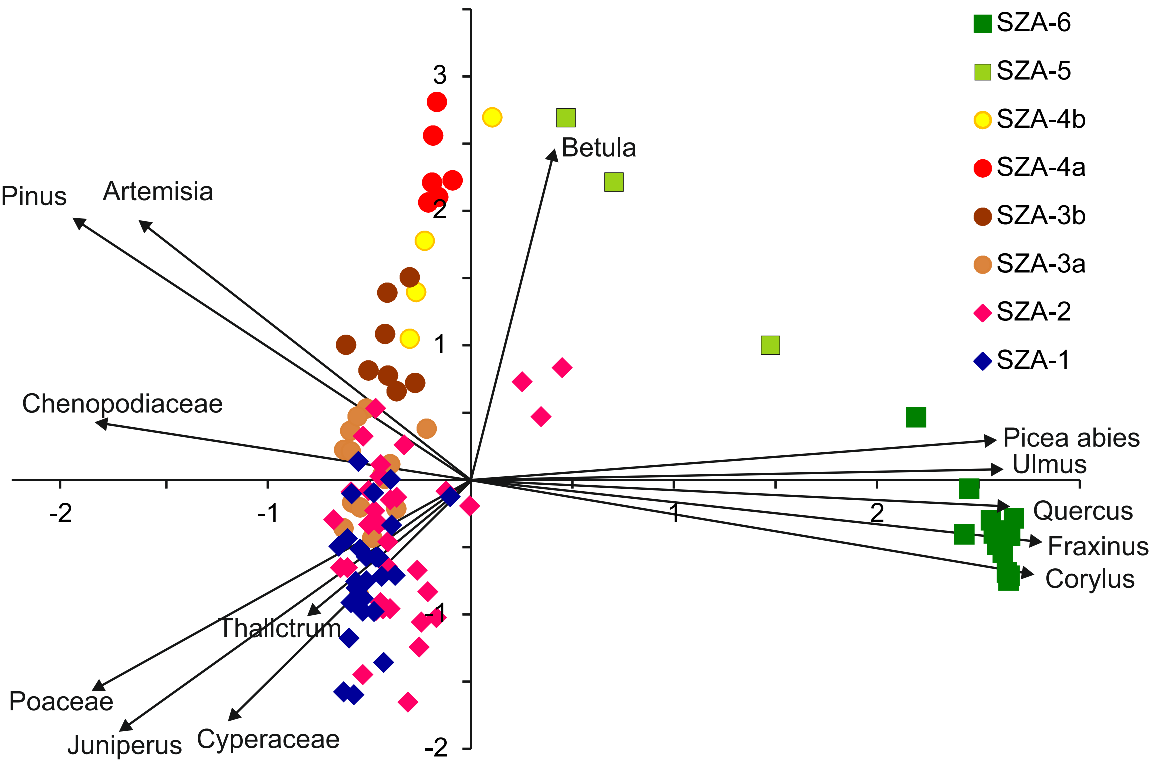
SZA-6
SZA-5
SZA-4b
SZA-4a
SZA-3b
SZA-3a
SZA-2
SZA-1
Betula
Pinus
Artemisia
Chenopodiaceae
Picea abies
Ulmus
Quercus
Fraxinus
Corylus
Thalictrum
Poaceae
Juniperus
Cyperaceae
3
2
1
-1
-2
-2
-1
1
2

Figure 08

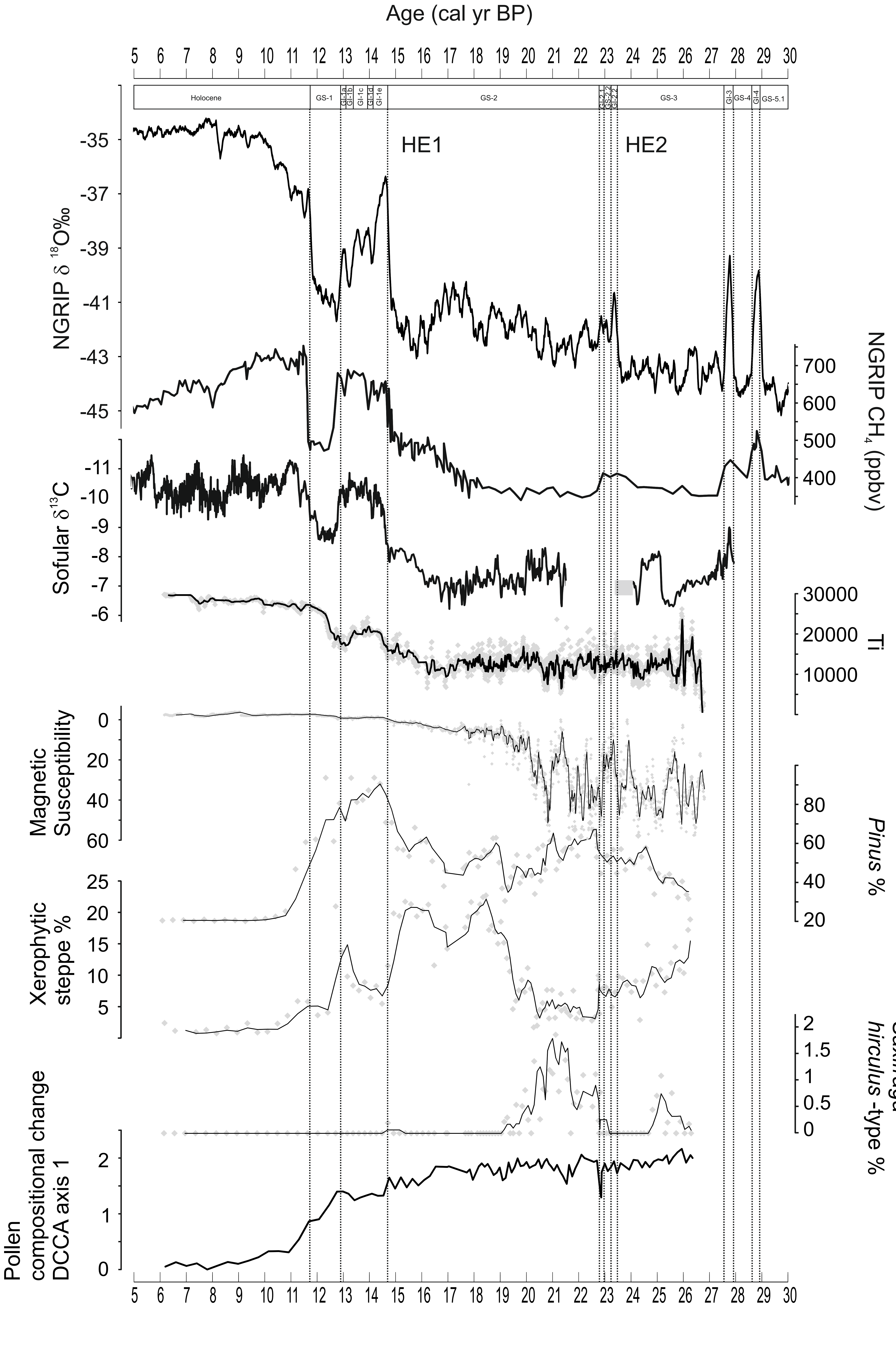

Age (cal yr BP)
Holocene
GS-1
GI-1a
GI-1b
GI-1c
GI-1d
GI-1e
GS-2
GS-3
GI-3
GS-4
GI-4
GS-5.1
HE1
HE2
NGRIP δ 18O‰
NGRIP CH4 (ppbv)
Sofular δ13C
Ti
Magnetic Susceptibility
Pinus %
Xerophytic steppe %
Saxifraga hirculus -type %
Pollen compositional change DCCA axis 1

Supplementary Figure 01

Click here to download Supplementary Data: Supplementary Figure 1.pdf

Supplementary Figure 02

Click here to download Supplementary Data: Supplementary Figure 2.pdf

Supplementary Figure 03

Click here to download Supplementary Data: Supplementary Figure 3.pdf

Supplementary Figure 4

Click here to download Supplementary Data: Supplementary Figure 4.pdf

Supplementary Table 01

Click here to download Supplementary Data: Supplementary Table 1.docx

Supplementary Table 02

Click here to download Supplementary Data: Supplementary Table 2.docx